Molecular insights into the role of heme in the transcriptional regulatory system AppA/PpsR.

Sofia Kapetanaki, Zsuzsanna Fekete, Pierre Dorlet, Marten Vos, Ursula Liebl, Andras Lukacs

▶ **To cite this version:**

Sofia Kapetanaki, Zsuzsanna Fekete, Pierre Dorlet, Marten Vos, Ursula Liebl, et al.. Molecular insights into the role of heme in the transcriptional regulatory system AppA/PpsR.. Biophysical Journal, 2022, 121, pp.2135-2151. 10.1016/j.bpj.2022.04.031 . hal-03658174

HAL Id: hal-03658174
https://hal.science/hal-03658174v1

Submitted on 7 Nov 2022

HAL is a multi-disciplinary open access archive for the deposit and dissemination of scientific research documents, whether they are published or not. The documents may come from teaching and research institutions in France or abroad, or from public or private research centers.

L'archive ouverte pluridisciplinaire **HAL**, est destinée au dépôt et à la diffusion de documents scientifiques de niveau recherche, publiés ou non, émanant des établissements d'enseignement et de recherche français ou étrangers, des laboratoires publics ou privés.

Molecular insights into the role of heme in the transcriptional regulatory system AppA/PpsR.

Running title
The regulatory role of heme in AppA/PpsR

Sofia M. Kapetanaki[1,2*#], Zsuzsanna Fekete[1], Pierre Dorlet[3], Marten H. Vos[4], Ursula Liebl[4], Andras Lukacs[1,2*]

[1] Department of Biophysics, Medical School, University of Pécs, 7624 Pécs, Hungary
[2] Szentagothai Research Center, University of Pecs, 7624 Pécs, Hungary
[3] Aix Marseille Univ, CNRS, BIP, IMM, Marseille, France.
[4]LOB, CNRS, INSERM, Ecole Polytechnique, Institut Polytechnique de Paris, 91128 Palaiseau Cedex, France
[#] Current Address: CEA–Institut de Biologie Structurale, Grenoble, 38044 France
*Correspondence: sofia.kapetanaki@ibs.fr, andras.lukacs@aok.pte.hu
Sofia M. Kapetanaki tel: +33 45 742 8623
Andras Lukacs tel: +36 72 53 5825

Abstract
Heme has been shown to have a crucial role in the signal transduction mechanism of the facultative photoheterotrophic bacterium *Rhodobacter sphaeroides*. It interacts with the transcriptional regulatory complex AppA/PpsR in which AppA and PpsR function as the antirepressor and repressor, respectively of photosynthesis gene expression. The mechanism, however of this interaction remains incompletely understood. In this study, we combined EPR spectroscopy and FRET to demonstrate the ligation of heme in PpsR with a proposed cysteine residue. We show that heme binding in AppA affects the fluorescent properties of the dark-adapted state of the protein, suggesting a less constrained flavin environment compared to the absence of heme and the light-adapted state. We performed ultrafast transient absorption measurements in order to reveal potential differences in the dynamic processes in the full-length AppA and its heme-binding domain alone. Comparison of the CO-binding dynamics demonstrates a more open heme pocket in the holo-protein, qualitatively similar to what has been observed in the CO sensor RcoM-2, and suggests a communication path between the BLUF and SCHIC domains of AppA. We have also examined quantitatively, the affinity of PpsR to bind to individual DNA fragments of the *puc* promoter using fluorescence anisotropy assays. We conclude that oligomerization of PpsR is initially triggered by binding of one of the two DNA fragments and observe a ~10-fold increase in the dissociation constant K_d for DNA binding upon heme binding to PpsR. Our study provides significant new insight at the molecular level on the regulatory role of heme that modulates the complex transcriptional regulation in *R. sphaeroides* and supports the two levels of heme signaling, via its binding to AppA and PpsR and via the sensing of gases like oxygen.

Statement of Significance

Controlling gene expression is a major challenge in the field of optogenetics underlying the need to explore new systems that can enhance its toolbox. The expression of the photosynthetic genes in *Rhodobacter sphaeroides* is regulated by two proteins, the light-sensing antirepressor AppA and the transcriptional repressor PpsR, making them attractive candidates in the control of cellular activities with light. However, the mechanism of regulation remains elusive. In this work, we provide mechanistic details on how heme - a well-known biological cofactor able to switch on/off the transcription of important proteins - can modulate the complex transcriptional regulation in *R. sphaeroides* via a two level signaling.

Introduction

Heme, a ubiquitous biological cofactor, is well known to switch on/off the transcription of important proteinous components (1, 2). In the so-called labile heme (LH) pools (3), a term used to refer to the pool of metabolically active cellular heme, the concentration, oxidation state, distribution, speciation and dynamics of LH remain poorly understood. Heme is insoluble in aqueous solutions and chaperones/transporter proteins (4-6) have been hypothesized to store and mobilize it within the cell for regulatory control. Such heme binding/storage proteins like bacterioferritin and heme chaperones like HemeW and glyceraldehyde-3-phosphate dehydrogenase have been recently identified to shuttle heme from its site of synthesis to target proteins (6,7). The subcellular distribution of LH is heterogeneous. Estimates for heme concentrations in the cell are in the range up to ~100 nM and can increase under certain conditions. In particular, reported LH concentrations vary from 20-40 nM for the cytosol, to below 2.5 nM for the mitochondria and the nucleus in the unicellular eukaryote *Saccharomyces cerevisiae* (8). In addition, signaling molecules like nitric oxide have been shown to mobilize LH resulting in a >10-fold increase in its concentration (8) whereas in a normal cell, the free heme concentration is considered to be below 10 μM (9).

The photosynthetic apparatus of the purple bacterium *Rhodobacter sphaeroides* is one of the proteinous components whose transcription can be switched on/off by heme. In *R. sphaeroides* heme constitutes one of the three major end products of the tetrapyrrole biosynthetic pathway, the other two being bacteriochlorophyll and vitamin B_{12}. The flow of tetrapyrroles in this trifurcated pathway is regulated by several transcriptional and post-transcriptional events that control their synthesis (10). Quantification of heme in *R. sphaeroides* has shown that there are in total 100,000-200,000 molecules per cell and an overall increase in heme levels per cell in oxygen-limited cultures compared to aerobic cells (11); yet the LH content has not been estimated. *R. sphaeroides* is a facultative photosynthetic bacterium. It employs the blue-light and redox-sensitive flavoprotein AppA (Activation of Photopigment and PUC A protein) to regulate the activity of the aerobic transcriptional repressor PpsR, which functions as a master regulator of photosynthesis development. Heme interacts with the transcriptional regulatory system AppA/PpsR and plays a key role in the formation of the photosynthetic apparatus. AppA/PpsR has been proposed to function as an oxygen-dependent transcriptional rheostat, fine-tuning the transcription of

photosynthesis genes as a response to changing oxygen concentration (12). At high oxygen level conditions, and at intense light conditions combined with low and intermediate oxygen levels, AppA/PpsR protects the cell from photooxidative damage by preventing the expression of the photosynthetic apparatus (13-16).

The flavoprotein AppA, which functions as an antirepressor of photosynthesis gene expression, consists of an N-terminal blue-light using flavin (BLUF) sensor domain (17-19) and an oxygen sensing containing heme instead of cobalamin (SCHIC) domain (12,20,21) (Fig. 1A). The light-adapted state of AppA is characterized by a rearrangement of the hydrogen bond around the flavin believed to be associated with conformational changes involving the β5 strand (Fig.1A). We have recently provided insight on the different conformational configurations of W^{104}, a crucial residue for downstream signalling in $AppA_{BLUF}$ that resides on the β5 strand (W^{104} is close to the flavin in the light-adapted state and away from the flavin in the dark-adapted state) (22). AppA is considered to integrate the two stimuli, light and redox, via its BLUF and SCHIC domains, respectively, and to communicate them to PpsR. PpsR is a well-known oxygen- and light-dependent repressor of bacteriochlorophyll, carotenoid and heme biosynthesis genes and *puc* operons (23).

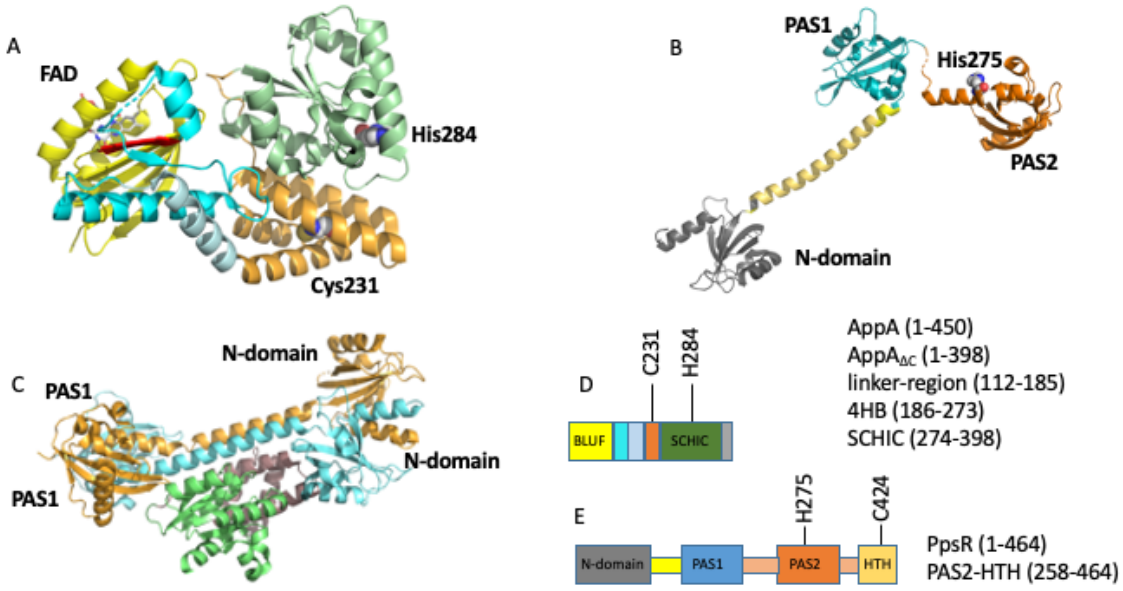

Fig. 1 (A) Structure of $AppA_{\Delta C}$ (pdb:4hh1) showing the BLUF domain (yellow), the linker region (cyan and light cyan), the 4HB domain (light brown) and the SCHIC domain (green). FAD, His^{284} and Cys^{231} are shown. The β_5 strand is shown in red. (B) Structure of one monomer of the dimeric PpsR without the HTH domain (pdb:4hh2). (C) Structure of the AppA-PpsR2 core complex (pdb:4hh3) showing the N- and PAS1-domain of PpsR (monomer 1: light blue and monomer 2: light brown) and the SCHIC domain of AppA (green) and 4HB (dirty violet). (D) Domain structure in AppA full-length, showing the BLUF (yellow), the linker region (cyan and light cyan), the 4HB (light brown), the SCHIC (green) and the Cys-rich (grey) domains. (E) Domain structure in PpsR showing the N- (grey), PAS1-(blue), PAS2-(orange) and HTH (ochre) domains. The residue numbers are shown for all constructs used as well as for the residues that ligate to heme iron.

The *puc* operon of *R. sphaeroides* comprises the *pucBA* structural genes, which encode B800-850 light-harvesting beta and alpha polypeptides, respectively (24). The *puc* promoter contains two PpsR binding sites (located 8 bp apart) required for repression *in vivo*. The consensus PpsR binding sequence is TGTc-N_{10}-gACA (lower case letters indicate lower conservation). PpsR is a multi-domain protein that consists of three PAS domains (N-terminal (N) domain, PAS1 and PAS2) (25,26), a glutamine-rich region (Q linker) and a helix-turn-helix (HTH) motif that binds the palindromic DNA (27) (Fig. 1B). Full-length PpsR exists in an oligomeric state that has already been described as either a dimer (26) or a tetramer (28) with a dynamic dimer-tetramer equilibrium ($2PpsR_2 \leftrightarrow PpsR_4$) and a K_d of 0.9 μM (29). The crystal structure of the protein reveals an intricate tetrameric assembly composed of two head-to-tail PpsR dimers. Both the N-terminal and the PAS1 domains form homodimers between which the alpha helical Q-linker forms a coiled coil-like structure that serves as binding site for the PAS2 domains of another PpsR dimer, leading to tetramer formation. However, the tetramer architecture alone cannot explain the highly cooperative DNA-binding mode observed for PpsR, because of the large distance between HTH-dimers that are separated by a half-turn of the DNA double helix. Active-site titration data and truncated PpsR proteins have supported a 1:8 stoichiometry of *puc*:PpsR binding (26,28,29). In the absence of a DNA-bound crystal structure for PpsR and based on the active site titration data and the DNA-bound crystal structure of the FIS protein (pdb: 3jre), a model for DNA binding to an octameric PpsR has been proposed (29). In that model, the alpha helical Q-linkers mediate interaction between symmetry-related tetramers enabling close positioning of two HTH dimers. PpsR binding to a 70 bp (*puc* I) or 250 bp (*puc* II) DNA fragment of the *R. sphaeroides puc* promoter displays cooperative binding (29) in line with previous findings (17). Eight PpsR molecules have been shown to saturate *puc* II, whereas four PpsR molecules are required for simultaneous binding to two different sites on DNA with an EC_{50}=1 μM and with looping out of the intervening DNA (29). This is not surprising as for the majority of helix-turn-helix-containing prokaryotic regulators the binding to palindromic sequences implies, the formation of a tetramer (30).

The SCHIC domain of AppA mediates the interaction with the transcriptional repressor PpsR (Fig. 1C) (12,20), forming an inactive AppA-$PpsR_2$ complex that dissociates upon illumination (17), although recent studies have argued against that assessment (29). An important aspect of AppA regulation is the binding of heme to the SCHIC domain (12,21). Heme has been shown to bind stronger to the dark-adapted state of AppA compared to the light-adapted state and to significantly reduce the length of the BLUF photocycle (21). Heme binds to the PAS2 and HTH domains of PpsR and induces conformational changes that are propagated to the covalently attached DNA binding domain, thus fine-tuning the accumulation of free tetrapyrrole. Heme therefore has been hypothesized to provide a mechanism for all characterized photosynthetic purple bacteria to respond to toxic free tetrapyrroles (31).

Whereas there are crystal structures of the SCHIC domain (21), AppA (29) and PpsR (29), there is no structural information on their heme-bound complexes. The mode of interaction of heme with the transcriptional regulatory system AppA/PpsR and its interplay with DNA binding are poorly

understood, and there are no studies on the interaction of PpsR with individual DNA sequences of the *puc* promoter. In this study, we provide novel information on the interaction of heme with these proteins using absorption, fluorescence and electron paramagnetic spectroscopies and demonstrate the ligation of heme in PpsR with a previously proposed cysteine residue. We have also probed the heme environment of AppA and PpsR using gaseous ligands, by studying their ligand binding dynamics. We present evidence for a weak interaction between the BLUF and SCHIC domains in AppA and provide quantitative information on the affinity of PpsR to labelled target DNA fragments and the effect of heme on DNA binding. Our study provides significant insight on important components modulating the complex transcriptional regulation in *R. sphaeroides*. Using this knowledge, we propose a model for the heme-based regulation.

Materials and methods

Materials

All chemicals were purchased from Sigma-Aldrich. Aqueous stock solutions of hemin for spectroscopic experiments were prepared by dissolving solid hemin in 0.1 M NaOH. Final concentration of stocks was calculated from the optical density at 385 nm (ε_{385} = 58.4 mM^{-1} cm^{-1}) (32).

Expression and purification of AppA$_{\Delta C}$, 4HB-SCHIC, PpsR, PAS2-HTH

The encoding *Rhodobacter sphaeroides* AppA without the Cys-rich domain, AppA$_{\Delta C}$ (residues:1-398), 4HB-SCHIC (residues:168-398) (Fig. 1D), full-length PpsR (residues:1-464), PAS2-HTH (residues:258-464) (Fig. 1E) were inserted into a pET-15b vector (Novagen) in frame with an N-terminal His_6-tag under control of a T7 promoter. A TEV site (GAAAACCTGTATTTTCAGGGC) was incorporated between the N-terminal His_6-tag and the coding sequences using the NEBuilder HIFI DNA Assembly Cloning Kit (NEB) in order to cleave the His_6-tag that could interfere with heme binding. Deletion of the Cys-rich domain in AppA has been shown to result in higher yields of soluble protein whereas to construct the SCHIC domain expression vector, the residues 168-398 were chosen in order to include the four-helix bundle (186-273) and a part of the linker region (168-185) (29). Inclusion of the four-helix bundle and a part of the linker region have allowed us to distinguish the effect of the BLUF domain alone in heme-binding to the SCHIC domain. Throughout the text we use the term 4HB-SCHIC for our SCHIC construct that contains the four-helix bundle and a part of the linker region and the term AppA$_{\Delta C}$ for the construct of AppA without the Cys-rich domain. The full-length PpsR (31) and the truncated PpsR variant PAS2-HTH that is able to bind heme and DNA were chosen for this study. All constructs were verified by DNA sequencing. Protein expression was performed using BL21(DE3) *Escherichia coli* cells. A single colony for each construct was used to inoculate 10 mL of Luria Broth (LB) media containing 10 µg/mL ampicillin. This culture was incubated at 37ºC overnight and was then used to inoculate 1 L of LB/ampicillin medium in a 4 L flask. The 1 L culture was incubated at 30ºC until the OD_{600} reached 0.4-0.5, after which the temperature was decreased to 18ºC for 30 minutes followed by addition of 0.8mM (0.2mM for 4HB-SCHIC) isopropyl-β-D-1-thiogalactopyranoside (IPTG) to induce protein expression. Both the expression

and purification of $AppA_{\Delta C}$ were performed in the dark. The cells were harvested by centrifugation (6000 rcf, 4ºC) and stored at -20ºC. The cell pellet was then resuspended in 40 mL of lysis buffer with 0.2mM phenylmethylsulfonyl fluoride (PMSF), DNase, protease inhibitor cocktail and lysozyme. The cells were lysed by sonication and cell debris was removed by centrifugation (39,000 rcf, 1hr). In the case of $AppA_{\Delta C}$, the supernatant was incubated with excess FAD (flavin adenine dinucleotide) for 45 min on ice in the dark. The supernatant was loaded onto a Ni-NTA (Qiagen) column which was washed with buffer containing 20 mM imidazole, the protein was eluted using 200 mM imidazole. The fractions containing proteins were pooled together, dialyzed and treated overnight with TEV protease to cleave the His_6-tag. PpsR and PAS2-HTH were also loaded onto a HiTrap heparin column and eluted with a NaCl gradient. All proteins were purified to homogeneity using size-exclusion chromatography (Superdex-200) and the purity of the final preparations was assessed by SDS-PAGE. All proteins were isolated as apo-forms. An SDS-PAGE analysis is presented in Fig. S1. Protein concentrations were estimated as shown in the Supporting Information. To obtain the absorption spectra of the heme bound complexes, the apoproteins were incubated for 15 min with substoichiometric hemin (~5 μM) in a ~6-10 fold excess of protein to maximize heme binding. That ratio was used for all measurements unless stated otherwise.
The following buffers were used for each protein: for $AppA_{\Delta C}$ and 4HB-SCHIC, lysis/wash buffer (20 mM Tris, 300 mM NaCl, 20 mM imidazole, 5% glycerol, pH 8.5), elution buffer (20 mM Tris, 300 mM NaCl, 200 mM imidazole, 5% glycerol, pH 8.5), for PpsR and PAS2-HTH, lysis/wash buffer (50 mM Tris, 300 mM NaCl, 20 mM imidazole, 10% glycerol, pH 8.0), elution buffer (50 mM Tris, 300 mM NaCl, 200 mM imidazole, 10% glycerol, pH 8.0).

Steady-state optical and fluorescence spectra

Absorption spectra were measured on a Perkin Elmer Lambda XLS+ and a Shimadzu 1700 spectrophotometer. Fluorescence emission spectra were obtained with a Horiba Jobin Yvon Fluorolog spectrophotometer using $\lambda_{exc} = 295$ nm as excitation wavelength. The applied slit width was set at 5nm for both the excitation side and the emission side. All fluorescence spectra were measured in the dark at 22ºC in a 10 mm x 1mm quartz cuvette.

EPR measurements

EPR spectra were recorded on an Elexsys 500 X-band spectrometer (Bruker) equipped with a continuous-flow ESR 900 cryostat and an ITC504 temperature controller (Oxford Instruments, Abingdon, UK). Experimental conditions: microwave frequency 9.48 GHz, microwave power 0.25 mW (T 15 K) or 1 mW (T 6.5 K), field modulation frequency 100 kHz, field modulation amplitude 2 mT, T 15K or 6.5K. Apoproteins (~120-140 μM) were incubated with substoichiometric hemin (final 100μM) for 15 min before freezing in liquid nitrogen.

Heme Binding Assays

Tryptophan fluorescence intensity was recorded from 500 nM $AppA_{\Delta C}$, PpsR, PAS2-HTH, and 800nM 4HB-SCHIC in 10mM Hepes, 100mM NaCl, 5% glycerol, pH 7.6. Heme that was prepared as described above was titrated to each protein and the Trp emission intensity was monitored as a function of heme concentration. Tryptophan fluorescence was observed using an excitation wavelength of λ_{exc} = 295 nm and the emission was measured between 300 and 550 nm. Dilution and inner field effects were taken into account in the data analysis. The wavelength λ=353nm, which gave the largest intensity changes between the protein and the heme-bound protein, was chosen for calculating the dissociation constant, K_d. K_d was obtained by plotting the corrected fluorescence intensity at each titration step against the concentration of heme and fitted to the Morrison (quadratic or tight-binding) equation (33) (equation 1) using the Origin 2020b software.

$$F_{obs}=F_0 + (F_{min} - F_0) * \frac{\left(C+x+Kd-\sqrt{(C+x+Kd)^2-4*C*x}\right)}{2*C} \quad \text{equation 1}$$

where F_{obs} is the observed fluorescence; F_0 is the initial fluorescence; K_d is the dissociation constant; C is the concentration of the protein; x is the total heme concentration. We note that for $C << Kd$ this expression approaches a hyperbolic curve.

Fluorescence Anisotropy-based DNA-binding Assays

Fluorescence anisotropy-based DNA binding assays with PpsR and PAS2-HTH were performed using 100 nM labeled DNA. Measurements were conducted at RT in buffer containing 10mM CHES pH 9, 10 mM NaCl and 15 % glycerol. A 19-mer and an 18-mer of double stranded DNA, corresponding to fragments of the PpsR promoter (27,31,34), and containing the putative binding site for PpsR were obtained by mixing equimolar amounts of the two complementary oligonucleotides 5′-TTGTCAGCCAACACTGACA-3′ (DNA1-forward) and 5′-TGTCAGTGTTGGCTGACAA-3′(DNA1-reverse) and 5′-TGTCAGCGCAATGTGACA-3′ (DNA2-forward) and 5′-TGTCACATTGCGCTGACA-3′ (DNA2-reverse) (Eurogentec). The 5′-extremity of the forward oligonucleotide was labeled with Texas Red. The oligonucleotides were heated 3 min at 80°C followed by slow cooling down to room temperature to allow complete annealing.

Fluorescence anisotropy measurements can provide useful information on the molecular size and the mobility of the fluorophore (35). Steady-state fluorescence anisotropy measurements were performed with a Fluorolog Jobin Yvon HORIBA spectrofluorometer in L-format configuration equipped with a polarization accessory. The measurements were performed at an excitation wavelength of λ_{exc} = 595 nm with a vertical polarization filter and by averaging the emission in the 610-630 nm range with the polarization filter both parallel and perpendicular with respect to the excitation light polarization. Fluorescence anisotropies were calculated from the fluorescence intensities detected according to the equation

$$r = \frac{I_v - 2G(\lambda)I_h}{I_v + 2G(\lambda)I_h}$$ equation 2

where r is the fluorescence anisotropy, I_v is the fluorescence emission intensity detected with vertical polarization, I_h is the fluorescence emission intensity detected with horizontal polarization and $G(\lambda)$ is the correction factor experimentally determined measuring the ratio I_v/I_h with a horizontally polarized excitation. Data processing was done using Origin 2020b and K_d values were determined by fitting a n=1 Hill equation.

Fluorescence anisotropy decay measurements.

Direct information on the orientational dynamics, which depend on the size and shape of the rotating species and on the fluidity of its microenvironment, can be obtained by analysis of the temporal decay of the anisotropy (35,36). $r(t)$ for an excited species in a single type of isotropic environment is given by a linear combination of exponentially decaying functions

$$r(t) = \sum_i \beta_i \exp(-\frac{t}{\theta_i})$$

where θ_i are the rotational correlation times and the sum of the factors β_i yields the initial emission anisotropy r_0.

Nanosecond time-resolved fluorescence measurements.

Time-resolved fluorescence measurements in the nanosecond time range were performed as previously described (22). To measure the fluorescence lifetimes, the excitation wavelength was set at 455 nm (FAD excitation) using a pulsed nanoLED (Horiba) with pulse duration 1.2 ns. The fluorescence emission was collected at 520 nm. The sample concentration was in the 5–10 μM range and 10 mm × 1 mm quartz cuvettes were used for the measurements. The integrity of the sample was monitored by UV-vis absorption spectroscopy before and after the fluorescence measurements, using a Thermo Scientific Evolution 600 UV-vis spectrophotometer.

Kinetic studies

The kinetics of heme dissociation from the ferric heme-complexes of $AppA_{\Delta C}$, 4HB-SCHIC, PpsR and PAS2-HTH were measured spectrophotometrically using a Jasco V-550 spectrophotometer. Transfer of hemin to myoglobin on reaction of the ferric heme-complexes (5 μM) with a 6-fold excess of apo-myoglobin (30 μM) was followed at 408 nm (experiments were carried out in 50 mM HEPES/ 50 mM NaCl pH 7.5).

Kinetic studies on PpsR and PAS2-HTH

The dissociation rate constant, k_{-CO}, for loss of CO from the ferrous heme-protein complexes of PpsR and PAS2-HTH was determined by ligand replacement (37). Typically, a mixture of 10% NO and 90% Argon was transferred to the headspace of an anaerobic cuvette containing the heme-protein-CO complex (300 µL, 5 µM). Release of CO was monitored by the rate of disappearance of the absorbance at 419 nm.

Stopped-flow experiments to monitor CO binding to the ferrous PAS2-HTH protein were performed in a Biologic SFM 300 instrument equipped with a J&M Tidas diode detector. The ferrous protein was prepared by addition of 0.5mM dithionite to the ferric protein to obtain the reduced non-liganded form (deoxy). The optical path length of the measuring cell was 0.8 mm. The instrument was extensively flushed with gaseous nitrogen prior to use. The instrument contains three reservoirs, containing protein solution (20 µM), saturated CO solution ([CO] = 1 mM (37) and anaerobic (oxygen-free) buffer. The mixing ratios for the experiments were chosen such that, after mixing, the protein concentration was 10 µM and the CO concentration varied (final concentration: 128, 193, 251, 386, 434 and 515 µM CO). The binding of CO to the protein was followed by recording the full spectra of solutions of the protein at various delay times.

Ultrafast spectroscopy

Apoproteins (~60 µM) were let to incubate with substoichiometric heme (~50 µM) for ~15 min in 50 mM HEPES/50 mM NaCl buffer, pH 7.5 to yield the heme-bound proteins solution. Experiments were performed in 1mm path length optical cells sealed with a gastight stopper. Oxygen was removed by several cycles of vacuum pumping and exposure to pure argon gas and the gas phase was subsequently replaced by 100% CO. The samples which were reduced with 0.5mM dithionite were left to equilibrate until formation of the Fe^{II}-CO complex was complete, as monitored by the steady-state absorption spectrum. Multicolour femtosecond absorption experiments were performed on a 500 Hz repetition rate setup as described (38), based on a Quantronix Integra-C Ti:sapphire oscillator/amplifier system, with a pump pulse centered at 570 nm and a broad band continuum probe pulse extending down to ~350 nm generated in a continuously translated CaF_2 window. Both test and reference probe beams pass through the sample, which is rastered with a Lissajous scanner. Data were globally analyzed in terms of multi-exponential decay using the Glotaran package (39).

Results

In order to obtain detailed insight into heme-protein interaction, besides the full-length PpsR protein, we have analysed truncated constructs of AppA and PpsR. These are $AppA_{\Delta C,}$ which does not include the C-terminal cysteine-rich domain (29), the heme-binding domain of AppA (SCHIC) that also incorporates the four-helix bundle (4HB-SCHIC) and a part of the linker region (29) (Fig.1D) and the truncated variant PAS2-HTH of PpsR which contains the two domains implicated

in heme binding (PAS2 and the HTH domain). The optical properties of the heme-bound complexes of all studied constructs and their heme association and dissociation constants are in agreement with the optical properties and dissociation constants of AppA, SCHIC and PpsR reported in previous studies (12,20,21,31) and are presented in the Supporting information (Fig. S2 and S3). In order to gain structural and functional information on the coordination of heme with each one of the components of the transcriptional regulatory system AppA/PpsR, we employed EPR spectroscopy and FRET measurements.

i) Characterization of the heme environment in AppA and PpsR by EPR spectroscopy

Our EPR measurements show heme binding to both $AppA_{\Delta C}$ and PpsR and in particular reveal the binding interactions with neighbouring residues.

The 15 K spectrum of the $AppA_{\Delta C}$-hemin complex consists of two sets of low-spin signals at g = (2.9, 2.2, 1.5) and g = (2.4, 2.2, 1.9) (Fig 2, left panel). The amount of the high-spin signal around g=6.0 is negligible as seen from experiments under conditions (T = 6.5 K, 1 mW) that enhance high-spin signals (Fig. 2, right panel). In contrast, in the 4HB-SCHIC domain the spectrum is characterized by a strong signal at g = 6.0 (Fig. 2) that is attributed to loosely bound high-spin ferric heme and a minor low-spin signal at g = (2.4, 2.2, 1.9). Figure 3 represent a Blumberg-Peisach correlation diagram (40). The rhombicity is plotted against the tetragonal field for a series of low-spin heme proteins and this defines empirically regions of similar axial ligands binding the heme cofactor. The more anisotropic EPR contribution of $AppA_{\Delta C}$ lies in the region corresponding to a bis-His ligation analogous to bovine liver cytochrome b_5. The less anisotropic component has the same g-values as 4HB-SCHIC and both lie in the region typical for Cys/His or Cys/OH ligation (41). The His^{284} residue (Fig. S4A) has been proposed as the axial ligand for heme binding in the SCHIC domain in AppA (21). Cys^{231} (Fig. S4A) is the only cysteine residue present in the helix bundle of the 4HB-SCHIC domain, pointing towards a His^{284}/Cys^{231} ligation for the ferric form in both proteins. However, the observed differences in heme binding to the 4HB-SCHIC domain compared to $AppA_{\Delta C}$ suggest that the BLUF domain can modify the conformation of the 4HB-SCHIC domain, affecting the coordination geometry of the heme iron, in line with the proposed weak interaction between the two domains (29). The identity of the His residues forming the bis-His complex is hard to determine. However, given the single K_{off} value for the heme transfer in the $AppA_{\Delta C}$ complex (see Table S3), we consider more likely His^{308} which is in the vicinity of His^{284} (Fig. S4B), to ligate with the heme iron.

The PpsR and PAS2-HTH/hemin complexes are characterized by low-spin signals at g = (2.4, 2.2, 1.9) due to Cys/His or Cys/OH^- ligation (Fig. 3) and the presence of a heme-bound high-spin species (g = 6.0) (Fig. 2). These findings identify Cys^{424} residue in the HTH domain as an axial ligand to the heme under oxidizing conditions, as previously proposed by optical spectroscopy and single-point mutations (31). Under reducing conditions both His^{275} (present in the PAS2 domain) (Fig. S4C) and Cys^{424} have been proposed to be the axial ligands (31). Table 1 summarizes the g values of the studied heme-bound protein complexes.

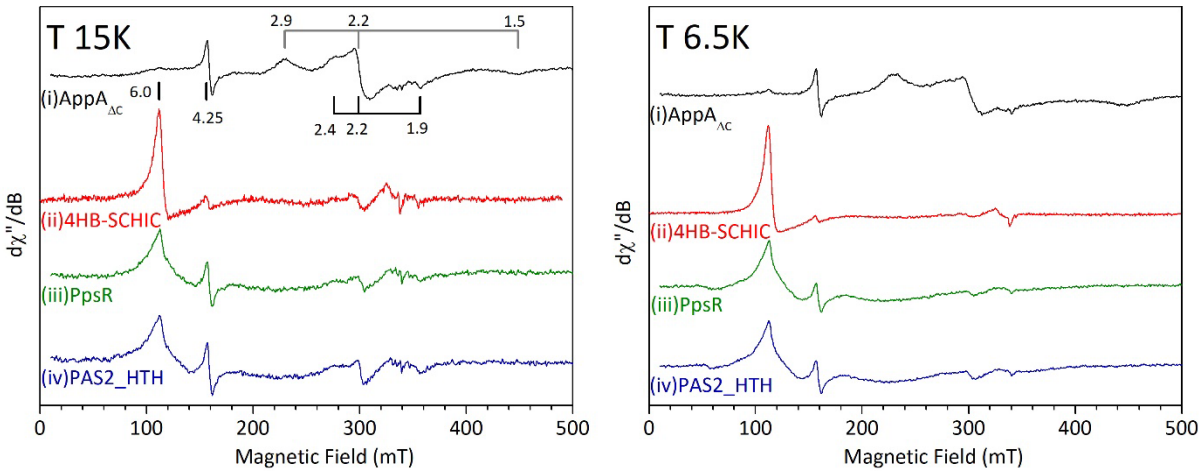

Fig. 2 X-band EPR spectra of (*i*) AppA$_{\Delta C}$-hemin complex, (*ii*) 4HB-SCHIC-hemin complex, (*iii*) PpsR-hemin complex, and (*iv*) PAS2-HTH-hemin complex at 15K (left panel) and at 6.5K (right panel). The signal at g=4.3 is due to rhombic iron contamination, minor Mn(II) contamination (6-line signal at g=2.00) is also visible. [heme]=100 μM.

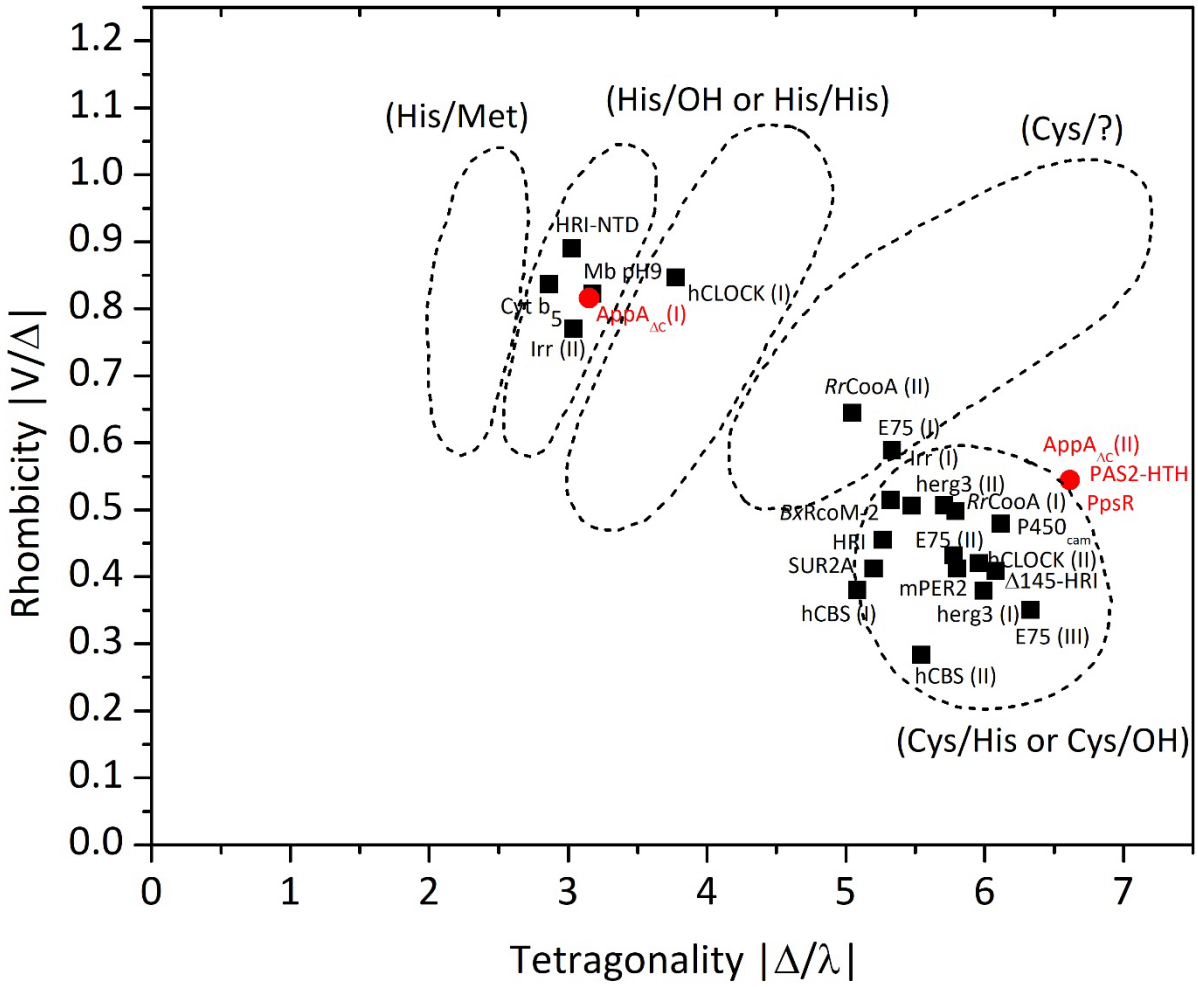

Fig. 3 Blumberg-Peisach correlation diagram for low-spin heme species (40). The data corresponding to the proteins studied here are shown in red along data corresponding to a series of previously characterized low-spin heme proteins (See Table S4) shown in black. The empirical regions delimiting a given type of axial heme ligation have been transposed from ref [40].

Table 1 Comparison of EPR g values of the studied proteins

Protein	**ligands**	***g values***			**crystal field parameters**		**References**
		g_z	g_y	g_x	$\|\Delta/\lambda\|$	$\|V/\Delta\|$	
$AppA_{\Delta C}$	His/His	2.9	2.2	1.5	3.1	0.8	this work
	Cys/His or Cys/OH^-	2.4	2.2	1.9	6.6	0.5	
PpsR	Cys/His or Cys/OH^-	2.4	2.2	1.9	6.6	0.5	this work
PAS2-HTH	Cys/His or Cys/OH^-	2.4	2.2	1.9	6.6	0.5	this work

ii) FRET measurements

To gain further insight on the location of the heme in both $AppA_{\Delta C}$ and PpsR, we took advantage of the fluorescent Trp residues in the proximity of the His residues (<30 Å) (Fig. S4) which bind heme as suggested by the absorbance (12,20,21,31) (Fig.S2) and our EPR results (Fig. 2).
A distance (~25Å) is observed between the only tryptophan residue (W^{302}) present in the heme-binding domain of AppA (pdb 4heh) and H^{284} that has been proposed to bind heme (Fig. S4A). PpsR has one tryptophan in the N-domain (W^{53}) and one tryptophan (W^{361}) in the PAS2 domain (Fig.S4C and S4E). The latter domain has been proposed to be involved together with the HTH domain in the interaction with heme, based on absorption studies (31). The distance between W^{361} and the histidine residue H^{275} that has been proposed to coordinate with the heme iron in reduced conditions is ~23Å (pdb 4hh2). Heme can act as a quencher of Trp fluorescence via Förster resonance energy transfer because the absorption spectrum of the heme overlaps with the emission spectrum of the tryptophan in the 300-420 nm region. Having estimated the Förster distance at which half the energy is transferred (R_0), we calculate Trp-heme distances R~30 Å for the 4HB-SCHIC domain, R~27 Å for PpsR and R~19 Å for the PAS2-HTH domain (see Supporting Information). These distances are in good agreement with the distances (Trp residue-His residue) obtained from the corresponding crystal structures, mentioned above and summarized in Table S2. Our FRET measurements, corroborate the findings from absorption spectroscopy (12,20,21,31) and our EPR results that implicate His^{275} and His^{284} as the heme ligands in PpsR and AppA, respectively. The small deviations between our FRET results and those estimated from the crystal structures are attributed to the fact that we measure distances between Trp and heme and not between Trp and His and the effect that other domains (4HB, N-terminal, PAS1) may have on the conformation of the heme-bound domain in AppA and PpsR.

iii) CO-binding dynamics in AppA and PpsR

Both AppA and PpsR heme-bound complexes have been reported to bind gaseous molecules like CO (carbon monoxide) and NO (nitric oxide) (12,31). We have further exploited this property using CO as a gaseous ligand in order to probe the heme environment and compare the dynamics of the full-length proteins with the heme binding domains alone in order to identify important features that control their function. The heme-CO bond can be photolyzed with high quantum yield and CO can escape from the heme pocket and eventually from the protein, or rebind directly to the heme. This dynamic behavior of CO rebinding can be followed by ultrafast transient absorption spectroscopy (42). Fig. 4A (inset i, ii and iii) shows the transient absorption spectra in the Soret band region for $AppA_{\Delta C}$ with the flavin reduced, or oxidized in the dark- and light-adapted states, at selected delay times after CO dissociation in the picosecond and early nanosecond time range. For the $AppA_{\Delta C}$ protein in all three cases, the heme-CO rebinding kinetics can be described by two phases with time constants of ~40 ps (30%), ~700 ps (40%) and the main non-decaying phase (30%). Clearly, the oxidation state of the flavin or the different light conditions do not seem to

affect the dynamics of CO rebinding to the heme in the SCHIC domain of the protein (Fig. 4B). Similar, but not-identical, kinetics was observed for the isolated 4HB-SCHIC protein which is characterized by two rebinding phases with time constants of ~50 ps (30%), ~900 ps (40%) and the main non-decaying phase (30%) (Fig. 4B).

The observation that the CO rebinding dynamics in the 4HB-SCHIC domain are similar to those of the full-length protein, is in line with the finding that in the full-length protein the redox or light conditions of the BLUF domain do not affect the ligand binding dynamics in the heme binding domain. The ligand binding dynamics in the heme binding domain are also not significantly affected by the absence or presence of the BLUF domain. Both the BLUF and the SCHIC domain have been shown to use the linker region and the 4HB as 'binding platforms' without strong interactions at their interface (29). The above results are in line with this feature. A comparison of the CO recombination parameters for the proteins of this study and other heme-proteins is provided in Table 2.

The insets in Fig. 4C show the transient absorption spectra in the Soret band region for PpsR and its truncated version PAS2-HTH at selected delay times after CO dissociation, in the picosecond and early nanosecond time range. The transient spectra, with a minimum around 420 nm and a maximum around 440 nm, reflect the formation of a 5-coordinate heme upon CO dissociation. Upon CO dissociation, CO located in the heme pocket can either rebind to the heme (geminate rebinding) or migrate out of the protein. CO partially recombines on the picosecond-nanosecond time scale as indicated by the decay of the amplitude of the transient spectra. Their shape also remains unchanged on this time scale suggesting that the spectral evolution reflects only CO rebinding to the heme and no formation of a 6-coordinate complex with two intrinsic residues. The kinetics for all PpsR complexes are characterized by a phase of a few picoseconds that reflects mostly photophysical processes (43) followed by multiphasic CO rebinding. For PpsR the latter process can be fitted with time constants of 100 ps (41%) and 1.4 ns (48%) and a non-decaying phase (11%) (Fig. 4C, inset i). In PAS2-HTH a multiphasic rebinding was also observed with time constants of 46ps (37%) and 660ps (48%) and a non-decaying phase (15%) (Fig. 4C, inset ii). Thus, substantially faster kinetics were observed in the case of the truncated protein PAS2-HTH suggesting that the N-terminal and PAS1 domain have an effect on the heme environment, in that they exert strain on the heme-binding pocket such that it becomes more open. Interestingly, qualitatively similar effects have been observed when comparing the full-length CO sensor RcoM--2 with its isolated heme domain (slower rebinding in the full-length protein) (44). A comparison of the ligand recombination kinetics for PpsR and PAS2-HTH is given in Fig. 4C.

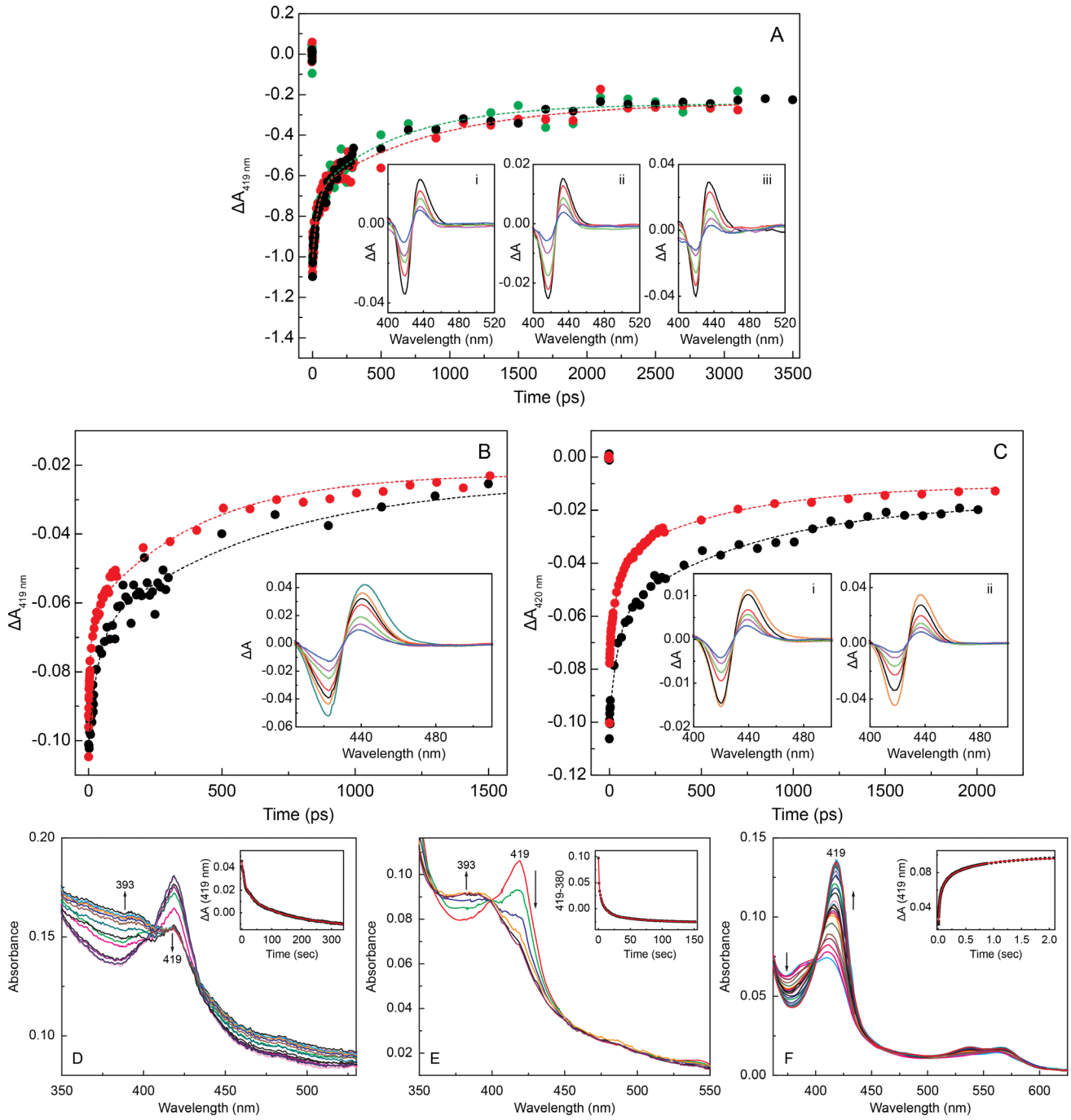

Fig. 4 (A) Comparison of the transients at 419 nm observed for the heme-CO complexes of flavin-oxidized $AppA_{\Delta C}$ in the dark-(black) and light- (green) adapted states and for the heme-CO complex of flavin-reduced $AppA_{\Delta C}$ (red). Inset i: transient absorption spectra of the heme-CO complex of oxidized $AppA_{\Delta C}$ in the dark-adapted state at various delay times after photodissociation of the CO ligand (2.3, 50, 200, 500, and 1700 ps). Inset ii: transient absorption spectra of the heme-CO complex of oxidized $AppA_{\Delta C}$ in the light-adapted state at various delay times after photodissociation of the CO ligand (2, 15, 100, 500, 2300 ps). Inset iii: transient absorption spectra of the heme-CO complex of reduced $AppA_{\Delta C}$ at various delay times after photodissociation of the CO ligand (3, 30, 200, 1300, and 3100 ps). (B) Comparison of the transients at 419 nm observed for the heme-CO complexes of oxidized $AppA_{\Delta C}$ in the light-(black) adapted states and for the heme-CO complex of the 4HB-SCHIC protein (red). Inset: Transient absorption spectra of the heme-CO complex of the 4HB-SCHIC protein at various delay times after photodissociation

of the CO ligand (5, 21, 46, 106, 406, 806, 1906 ps). **(**C) Comparison of the transient absorption at 420 nm observed for the heme-CO-PpsR (black) and heme-CO-PAS2-HTH complex (red) after photodissociation of the CO ligand. Inset i. Transient absorption spectra of the heme-CO-PpsR complex at various delay times after photodissociation of the CO ligand (1.3, 6, 106, 226, 506, and 1106 ps). Inset ii. Transient absorption spectra of the heme-CO-PAS2-HTH complex at various delay times after photodissociation of the CO ligand (1.2, 20, 100, 300, 900, and 2500 ps). (D) Kinetics and spectral changes associated with dissociation of CO from the ferrous heme-PpsR complex and (E) from the ferrous heme-PAS2-HTH complex in the presence of NO. The insets show the 419 nm time traces, along with exponential fits. (F) Stopped-flow spectra recorded on binding of CO (515 μM) to the ferrous PAS2-HTH-heme complex (10 μM).

Table 2 Parameters of CO recombination in heme proteins.

Protein	**Recombination time constants/ps (rebinding fraction)**	**Non-decaying phase**	**References**
PpsR	100 (41%), 1400 (48%)	11%	this work
PAS2-HTH	46 (37%), 660 (48%)	5%	this work
$AppA_{\Delta C}$	40 (30%), 700 (40%)	30%	this work
SCHIC	50 (30%), 900 (40%)	30%	this work
CooA	78 (60%), 386 (30%)	10%	(45,46)
DNR	100 (30%), 900 (35%)	35%	(47)
E. coli DOSH	1500 (60%)	40%	(48)
E. coli DOS	1600 (64%)	36%	(49)
FixL	0 (0%)	100%	(50)
R220H FixL	280 (25%), 2400 (35%)	40%	(51)
RcoMH-2	170 (65%), 500 (35%)	0%	(52)
RcoM-2	180 (45.3%), 660 (54.1%)	0.6%	(44)
$SUR2A^{615-933}$	22 (14%), 150 (26%), 2500	10%	(53)

CooA: CO Oxidation transcriptional Activator from Rhodospirillum rubrum, DNR: Dissimilative Nitrate Respiration Regulator/transcription factor from Pseudomonas aeruginosa, DOS: Escherichia coli Direct Oxygen Sensor (full-length), DOSH: the heme binding domain of DOS, FixL: transcriptional activator of nitrogen fixation, RcoM-2: Regulator of CO Metabolism (full-length), RcoMH-2: the heme binding domain of RcoM-2, SUR2A: sulphonylurea receptor subunit, a member of the ATP-binding cassette transporter superfamily

We have further determined the CO dissociation rates from the ferrous-heme CO complexes of PpsR and PAS2-HTH by measuring the time courses for the replacement of bound CO by NO (37). Addition of 10% gaseous NO results to a gradual decrease of the Soret band of the CO-bound complex (420 nm) with a concomitant increase of an absorbance at ~390nm (Fig. 4D and Fig. 4E). Approximately 27% of a heme-NO-PpsR complex forms with a rate of 0.15 s^{-1}, 27% forms with a rate of 0.04s^{-1} and 46% forms with a rate of 0.006 s^{-1} (Fig. 4D). In the case of the truncated protein, PAS2-HTH, 43% of the PAS2-HTH –heme NO complex forms with a rate >1s^{-1}, 39% forms with

a rate of 0.15 s^{-1} and 18% forms with a rate of 0.023 s^{-1} (Fig. 4E). These values are in the same range observed for other sensor heme proteins (53). The differences observed between the full-length and the truncated PpsR point towards differences in the heme environment attributed to the presence of the N-terminal and PAS1 domains, as also suggested by the CO-rebinding dynamics. Interestingly, the absorption spectra of the NO-bound species are dominated by a Soret band at ~393nm which is consistent with a 5-coordinate NO-bound species, observed in many sensor heme systems (53-59). The formation of a 5-coordinate NO-bound PpsR species hasn't been reported earlier and it suggests lability of the intrinsic proximal heme ligand.
We employed stopped-flow spectroscopy to study the binding of CO to the ferrous-heme PAS2-HTH domain. In the presence of CO, a heme-CO complex is formed which consequently binds to the protein forming the PAS2-HTH-heme-CO complex (Fig. 4F). The CO binding kinetics are highly multiphasic, suggesting considerable heterogeneity.

iv) Heme-induced changes in the flavin fluorescence properties of the BLUF domain

Since blue-light irradiation results in the reorganization of the H-bond network around the flavin, that are transmitted through the C-terminal domain of the protein to partner binding proteins, it is important to know whether, reversely, heme binding in the C-terminal domain has also an effect on the flavin environment. Indeed, heme binding to $AppA_{\Delta C}$ in the dark-adapted state results in an increase and red-shift, from 505 to 517 nm, of the flavin fluorescence (Fig.5A). Such a red-shift is also qualitatively observed upon treatment of $AppA_{\Delta C}$ with guanidinium chloride (a chemical agent known to denature proteins) (Fig. S5), which is accompanied by the release of the flavin as indicated by the emission maximum at 523nm. These results suggest that in heme-bound $AppA_{\Delta C}$, flavin is present in an environment with less H-bonding, and is hence more flexible, compared to $AppA_{\Delta C}$ without heme. To characterize further the flavin environment in the heme-bound $AppA_{\Delta C}$, we applied TCSPC (time-correlated single photon counting) and time-resolved fluorescence anisotropy decay measurements. Fig.5B shows the fluorescence decay of the dark-adapted $AppA_{\Delta C}$ in the absence and presence of heme. Heme binding to $AppA_{\Delta C}$ results to a substantial increase of the average fluorescence lifetime of the flavin from ~2ns (heme-free $AppA_{\Delta C}$) to 4.4 ns (heme-bound $AppA_{\Delta C}$) (Table S5). The latter value is in the same range as the fluorescence lifetime of flavin in solution (~3-5ns) (60-62) and suggests that the fluorescence of the flavin in heme-bound $AppA_{\Delta C}$ is not quenched by adjacent amino acid residues, but that the flavin is exposed to the solvent. In line with the fluorescence lifetime measurements, the rotational correlation time of the flavin in the dark-adapted $AppA_{\Delta C}$ drops dramatically in the presence of heme, $\tau_h = 0.8 \pm 0.1$ns, compared to the absence of heme, $\tau = 4.1 \pm 1.4$ ns (Fig. 5C) (Table S6). Fast rotational correlation times (~1 ns) suggest a fast movement of the fluorophore (35) and support the hypothesis that the flavin is exposed to the solvent and hence has some rotational freedom. The value obtained however, reflects the movement of a flavin chromophore that is still bound, as the rotational correlation time of free flavin is ~ 0.24 ns (63). By contrast longer correlation times (up to tens of ns) may reflect a slower rotation of the fluorophore or the entire protein complex (35).

Hence, overall, the above fluorescence measurements point towards a flavin present in a flexible environment in the dark-adapted state.

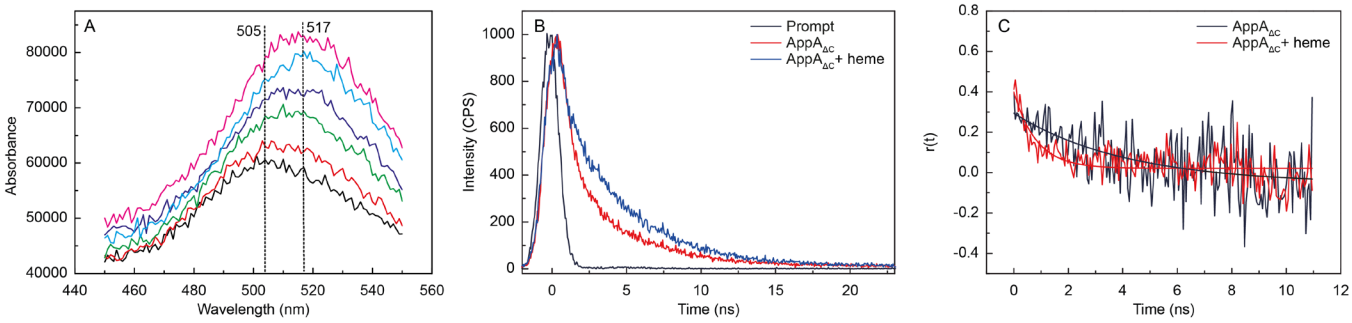

Fig. 5 (A) Shift of the fluorescence emission maxima of the dark-adapted AppA$_{\Delta C}$ at increasing heme concentrations. (B) Fluorescence decay of the dark-adapted AppA$_{\Delta C}$ in the absence (red) and presence of heme (blue) after excitation at 455 nm, (λ_{em} = 520 nm). The instrument response function (~ 1 ns) is shown in black. (C) Decay of the fluorescence anisotropy of the dark-adapted AppA$_{\Delta C}$ in the absence of heme (black) and in the presence of heme (red). Fits are shown as solid traces.

v) Binding of PpsR and the PpsR-heme complex to DNA.

The carboxyl terminus of PpsR, containing the HTH domain that binds to the palindromic motif TGTcN$_{10}$gACA is responsible for the repressor activity of the protein (23). As previous studies have not examined the effect of a single palindrome sequence, we have used two different DNA sequences of the *puc* promoter where only one palindrome is present per sequence in order to examine the effect of each one of the two palindromes that bind to the DNA binding sites of PpsR. As heme-binding affects the interaction between PpsR and its target DNA, we carried out quantitative DNA-binding assays based on fluorescence anisotropy to determine the affinity of the PpsR repressor for the two palindromic sequences of the *puc* promoter. The two double stranded DNA fragments that we used, DNA1 and DNA2 (Fig. S4F), correspond to fragments of the PpsR promoter (27,31,64) and contain the putative binding site for PpsR. Addition of PpsR and PAS2-HTH to labelled DNA increases the fluorescence anisotropy of the Texas Red label because DNA binding to the proteins results in an increase of the volume of the labelled entity and hence slows down its rotational movement.

In the absence of heme, we determined a binding constant for DNA1 (K_d) of 0.9 ±0.2 µM for PpsR (Fig. 6A) and 1.25 ±0.23 µM for PAS2-HTH (Fig. 6B). For both cases, in the presence of the heme a lower asymptotic anisotropy was observed. This implies that the rotation time for protein-bound DNA1 was shorter, suggesting a weaker interaction with the proteins which is in line with previous findings (31). Furthermore, the K_d was significantly higher in the presence of heme (8.5 ± 0.7 µM for PpsR-heme and 12.2 ± 1.1 µM for PAS2-HTH-heme) indicating weaker binding of DNA1 due to the interaction of the heme molecule with the proteins. Binding of oxidized AppA$_{\Delta C}$ to PpsR does not seem to affect significantly the binding of DNA1 (K_d= 2.0 ± 0.3 µM) in line with previous

studies (20) where only the reduced form of AppA was found to function as an antirepressor of PpsR (Fig. 6A) (17). As a control, we examined DNA1 binding to oxidized $AppA_{\Delta C}$ and we observed no binding, as expected (Fig. 6A). Binding of DNA1 also is not affected by reducing PpsR (1mM DTT that reduces the disulfide bridge, C^{424}-C^{251} (28)) (K_d=1.0 ±0.3 μM) or by heme binding to reduced PpsR (K_d=1.0 ±0.3 μM) (Fig. 6C).

Similarly, we determined the affinity of PpsR for the DNA2 sequence at 5.3 ± 2.6 μM (K_d) which indicates weaker binding of DNA2 (Fig. 6D) to the protein compared to DNA1 (Fig. 6A). A weaker affinity for the DNA2 sequence was also determined for PAS2-HTH (K_d = 16 μM). In the presence of heme for both proteins the anisotropy of DNA2 is significantly lower, suggesting a very weak binding (Fig. 6D-E). Binding of PpsR to DNA2 is not affected significantly by oxidized $AppA_{\Delta C}$ binding to PpsR, whereas $AppA_{\Delta C}$ does not interact with DNA2, as expected (Fig. 6D).

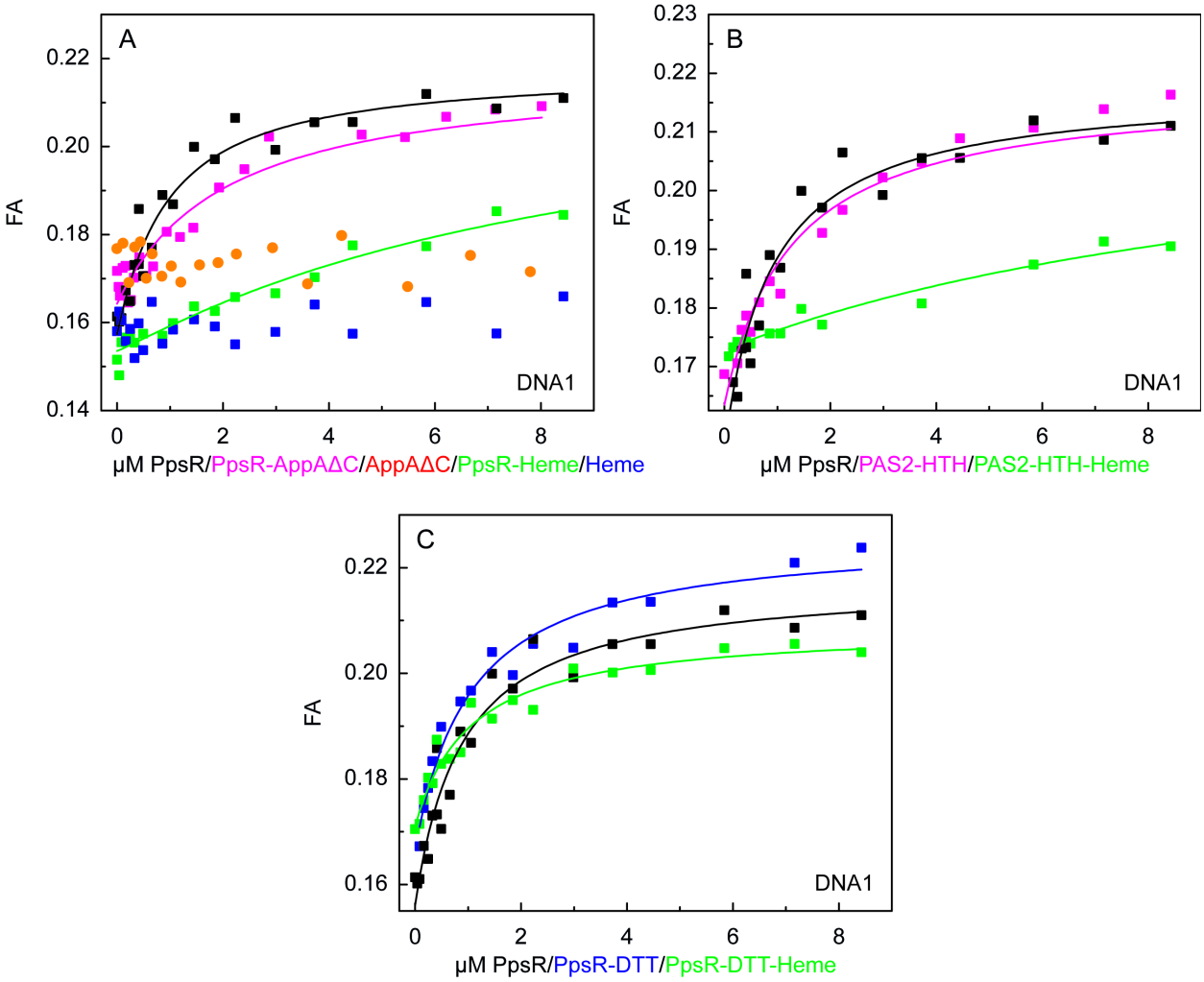

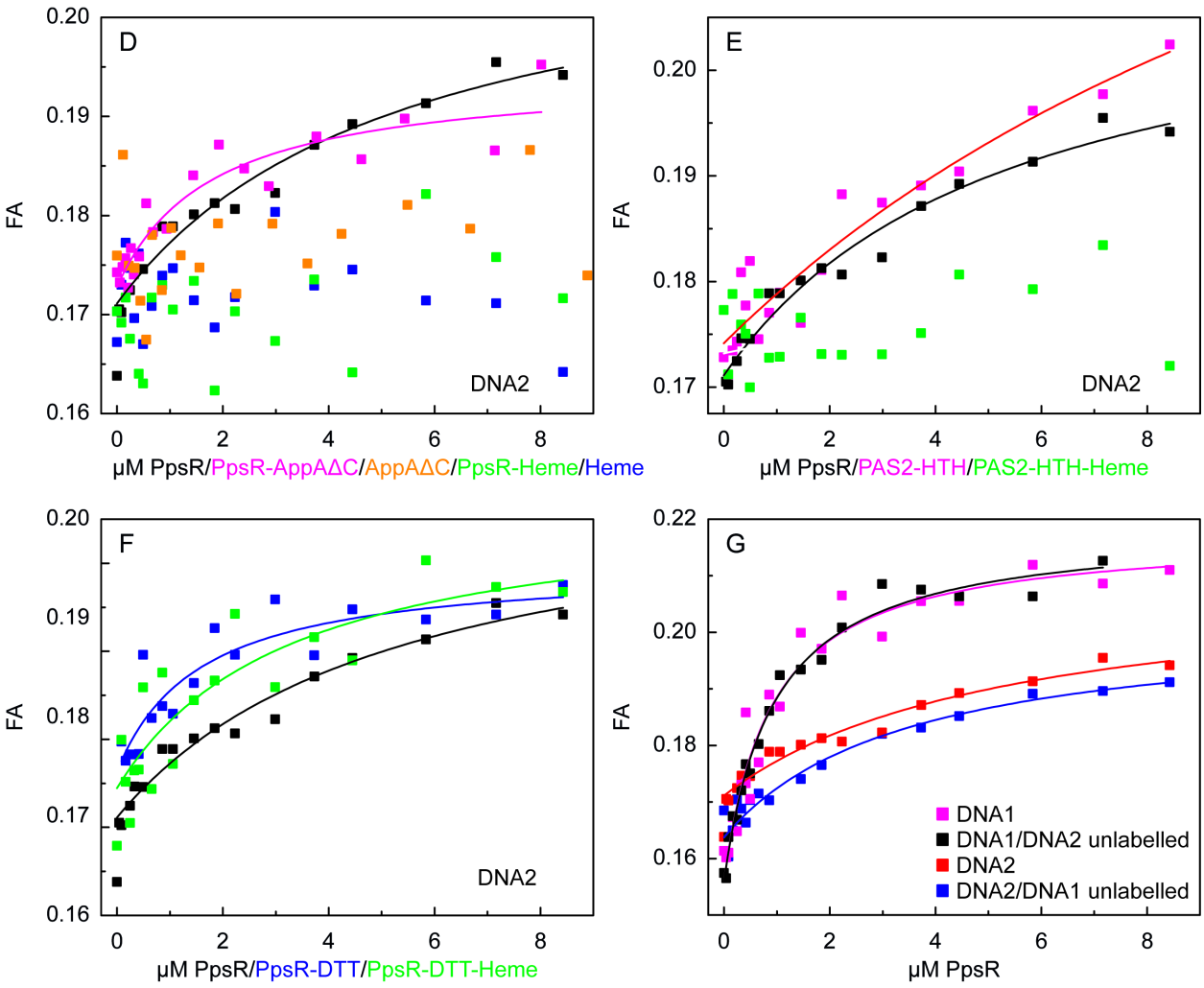

Fig. 6 Texas Red labelled DNA is used in all cases and is referred hereafter as DNA (A) Binding of PpsR and its complex with $AppA_{\Delta C}$ and heme to DNA1 determined by fluorescence anisotropy. Binding of DNA1 is also shown for $AppA_{\Delta C}$ and heme (control). (B) Binding of PAS2-HTH and its complex with heme to DNA1 determined by fluorescence anisotropy. (C) Binding of reduced PpsR and reduced PpsR-heme to DNA1 determined by fluorescence anisotropy. (D) Binding of PpsR and its complex with $AppA_{\Delta C}$ and heme to DNA2 determined by fluorescence anisotropy. Binding of labelled DNA2 is also shown for $AppA_{\Delta C}$ and heme (control). (E) Binding of PAS2-HTH and its complex with heme to DNA2 determined by fluorescence anisotropy. (F) Binding of reduced PpsR and reduced PpsR-heme to DNA2 determined by fluorescence anisotropy. Fitting to the binding curves is shown by solid lines. (G) Comparison of the binding of PpsR to DNA1 (DNA2) (100nM) in the presence of unlabeled DNA2 (DNA1) (500nM).

These findings are similar to those observed for DNA1 as outlined above. A slightly different binding affinity was determined for DNA2 upon reducing PpsR (1mM DTT) (K_d= 1.6 ± 0.9 μM) which was not significantly affected by the presence of heme (K_d= 3.3 ± 2.8 μM) (Fig. 6F). All results are summarized in Table 3.

Five-fold excess of unlabeled DNA2 or DNA1 in the presence of labelled DNA1 or labelled DNA2, respectively, did not result to significant changes in the affinity compared to the absence of unlabeled DNA (Fig. 6G). This implies that, in the nanomolar concentration range, no effective competition for the same binding sites occurs. This finding suggests that despite the same consensus sequence TGTcN$_{10}$gACA of DNA1 and DNA2, protein binding to DNA is rather specific due to the different N10's. However, binding of DNA1 to the binding site1 of PpsR is stronger (K_d= of 0.9 ±0.2 μM) (Fig. 6A) compared to binding of DNA2 to the binding site2 of PpsR (K_d=5.3 ± 2.6 μM) (Fig. 6D).

Table 3. Dissociation constants for DNA binding to PpsR.

Protein	K_d for DNA1 (μM)	K_d for DNA2 (μM)
PpsR	0.9 ± 0.2	5.3 ± 2.6
PAS2-HTH	1.25 ± 0.23	16 ± 15
PpsR-heme	8.5 ± 0.7	
PAS2-HTH-heme	12.2 ± 1.1	
PpsR-AppA	2.0 ± 0.3	
PpsR/DTT	1.0 ± 0.3	1.6 ± 0.9
PpsR/DTT-heme	1.0 ± 0.3	3.3 ± 2.8

Discussion

Weak heme binding to AppA and PpsR is modulated by Cys residues

Previous studies aiming to investigate the heme environment in AppA and PpsR were limited to the application of point mutations and absorption spectroscopy to shed light on the identity of the residues coordinating to the heme iron. In AppA, Cys^{231} in the 4HB-SCHIC domain and the highly conserved - based on sequence alignments of the SCHIC and B$_{12}$-binding domains -residue, His^{284} have been proposed as axial ligands (12,21). A His/Cys ligation is suggested from the EPR spectra of AppA$_{\Delta C}$ pointing towards a ligation to Cys^{231} which is the only cysteine residue in the 4HB-SCHIC domain (heme-binding domain). Additional evidence for the involvement of His^{284} and His^{275} as the heme ligands in AppA$_{\Delta C}$ and PpsR, respectively, arise from our FRET measurements in which the estimated distances are in line with the estimated distances from the crystal structures (Table S2). Similarly, a His/Cys ligation characterizes also the heme sensor HRI (heme-regulated eIF2α kinase), whereas in the truncated protein Δ145-HRI that lacks the His residue, heme iron ligates to a Cys and H_2O/OH^- ligand (65). These findings favor our assignment to a His/Cys ligation in view of the His residues (His^{284} and His^{275}) present in the proteins.

In PpsR, Cys^{424} in the HTH domain has been proposed as the axial ligand under oxidizing conditions whereas under reduced conditions both His^{275} and Cys^{424} have been proposed to be the axial ligands (21). In this work, using EPR spectroscopy and FRET measurements we provided further insights on the coordination environment of the heme iron. Our EPR measurements on

PpsR are in line with a Cys ligation in the ferric state. A cysteine thiolate is a well-known critical group found in many proteins that function as heme sensors. It displays weak coordination to the Fe(III) heme complex and even weaker to the Fe(II) heme complex if it is not supported by another proximal residue. The origin of this redox effect is the stronger electrostatic repulsion due to the largest number of electrons in the Fe(II) heme complex compared to the Fe(III) heme complex (66).

The K_d values calculated from our measurements for Appa$_{\Delta C}$ and 4HB-SCHIC (K_d=0.5 ± 0.1 μM for AppA$_{\Delta C}$ (dark), K_d=0.15 ± 0.05 μM for AppA$_{\Delta C}$ (light)) and 0.6 ± 0.1 μM for 4HB-SCHIC) are similar to the value (K_d=1.2 ± 0.4 μM) reported for the full-length AppA (12). For PpsR and its truncated version PAS2-HTH, we obtained K_d values of 3.9 ± 1 μM and 4.7 ± 0.7 μM, respectively which are in line with the K_d of 1.9 μM that has been reported previously from fluorescence quenching measurements for PpsR (31). These K_d values are all similar and indicative of weak binding of the heme ligand and are in line with a regulatory role of the heme as described in several systems involved in transcription (1). All results are summarized in Table S3. It should be noted that whereas our tryptophan fluorescence quenching measurements (Fig. S3B) and absorption measurements (Fig. S2C) clearly demonstrate heme binding to the light-adapted state of AppA, it has been suggested that this does not occur based on single-wavelength stopped-flow measurements (21).

Heme binding to the 4HB-SCHIC domain of the dark-adapted AppA$_{\Delta C}$ induces conformational changes in the BLUF domain

A weak interplay between the BLUF and SCHIC domains has been proposed based on the crystal structure of AppA$_{\Delta C}$ that lacks a strong interaction at the BLUF-SCHIC interface of AppA$_{\Delta C}$. The BLUF and the SCHIC domain are interconnected via a linker region and a 4HB that serve as 'binding platforms' (29). Our EPR and fluorescence spectroscopy studies provide evidence for this type of weak interaction. In particular, the heme-bound AppA$_{\Delta C}$ and heme-bound 4HB-SCHIC domain are characterized by different coordination geometries to the heme iron (Fig. 2), suggesting that the presence of the BLUF domain can modify the conformation of the 4HB-SCHIC domain. On the other hand, heme binding to the 4HB-SCHIC domain of the dark-adapted AppA$_{\Delta C}$ affects the fluorescent properties of the flavin in the BLUF domain. Notably, we observed a substantial change in the environment of the flavin to a more flexible conformation where the flavin is more exposed as indicated by the red-shift of the emission spectrum (Fig. S3A), the increase of the fluorescence lifetime (Fig. 5B) (Table S5) and the decrease of the rotational correlation time of the flavin in the heme-bound dark-adapted AppA$_{\Delta C}$ (Fig. 5C) (Table S6). In addition, the photocycle of the heme-bound AppA has been shown to be significantly reduced (decay half-life ~4 min) compared to AppA without heme (decay half-life ~15 min) (21). These findings illustrate clearly the weak interconnectivity between the two domains in AppA.

Interestingly, while heme binding to the dark-adapted AppA$_{\Delta C}$ has an effect on the flavin environment as mentioned above and indicated by the changes in the fluorescent properties of the protein, this is not the case for the heme-bound light-adapted AppA$_{\Delta C}$ (Fig. S3B). The light-

adapted state of AppA is characterized by a rearrangement of the hydrogen bond around the flavin believed to be associated with conformational changes involving the β5 strand (Fig.1A). We have recently observed different conformational configurations in the light-adapted and dark-adapted states of $AppA_{\Delta C}$ for W^{104}, a crucial residue for downstream signalling in $AppA_{BLUF}$ which resides on the β5 strand. We found that W^{104} is close to the flavin in the light-adapted state and away from the flavin in the dark-adapted state (22). Based on these findings, we propose that in the light-adapted state, the flavin environment is arranged in such a way that changes in the 4HB-SCHIC domain due to heme binding cannot be transmitted. By contrast, in the dark-adapted state, heme binding has an effect on the flavin environment as indicated by the changes in the fluorescent properties of the protein. These findings are in line with the current view that AppA integrates two stimuli (light and redox) (21).

Ligand binding dynamics reveal allosteric interactions in both AppA and PpsR

Addition of oxygen to ferrous heme-bound AppA has been shown to discoordinate heme instead of forming a long-lived oxy complex (12). However, both AppA and PpsR in their heme-bound complexes have been reported to bind gaseous molecules like CO (carbon monoxide) and NO (nitric oxide) (12, 31) as also demonstrated by our measurements (Fig. 4 and Fig. S2). We have further exploited this property using CO as a gaseous ligand in order to probe their heme environment. Photodissociation of the heme-CO bond and subsequent monitoring of the spectroscopic changes occurring upon heme-CO re-ligation provide an exquisitely sensitive probe of the heme-iron environment and allow characterizing the intraprotein migration of that diatomic gaseous molecule. Analysis of the dynamics of CO binding and escape provides insight into how the pathway of the dissociated ligand is controlled by the protein environment (67). We observed multiphasic CO recombination in both proteins, suggesting considerable heterogeneity on the timescale up to a few nanoseconds. In $AppA_{\Delta C}$, there is a substantially higher escape of the CO ligand from the heme pocket in the nanosecond timescale than in PpsR, suggesting a more flexible environment and/or ligand access pathway. Considering that AppA has been suggested to act as an oxygen sensor (12), such a pathway would be necessary for the entry and exit of the oxygen molecule. The presence or absence of the BLUF domain does not seem to affect the CO rebinding in the 4HB-SCHIC domain, under conditions where heme is reduced. On the contrary, as suggested by our EPR data (Fig. 2), the presence or absence of the BLUF domain seems to affect the binding of ferric heme iron to the 4HB-SCHIC domain. The reverse is apparently possible as the ferric heme-binding to the 4HB-SCHIC domain seems to influence the flavin environment in the dark state (Fig. S3A). Together these findings suggest that the redox state of the heme iron may play a role in the transduction mechanism between the BLUF and the SCHIC domain. Finally, slightly different CO recombination kinetics are observed between the holo-protein and its truncated version in PpsR, suggesting an effect of the N-terminal domain and the PAS1 domain on the local heme environment. Qualitatively, such effects have been observed previously in a bacterial CO-sensor heme protein (44). Whether these differences between the full-length protein and the truncated version of PpsR are due to the absence of the putative disulphide bridge (Cys^{251}-Cys^{424})

(28) in the PAS2-HTH or another conformational change that affects the heme environment remains to be investigated. These findings are in general agreement with allosteric interactions that need to occur in both proteins in order for a light-signalling pathway to take place and point to the proposed cooperativity given the ternary AppA-PpsR-DNA complex that is formed (17).

Binding of PpsR to DNA

Gas-controlled heme binding transcription factors have been shown to display high affinities (in the nM range) to DNA (44 nM for DNR, <2 nM for RcoM-2) and 8nM for CooA (44,47,68). In our studies, only one PpsR molecule is implicated in binding each palindrome (Hill coefficient n=1). We found that DNA1 binds with higher affinity to PpsR (K_d =0.9 ±0.2 μM) compared to DNA2 binding to PpsR (K_d =5.3 ± 2.6 μM). In the presence of 5-fold excess of unlabelled DNA, we did not observe changes in the binding affinity which suggest that the two DNA sequences are specific for their binding sites (Fig. 6G). The estimated affinities of DNA to PpsR are in the same order of magnitude as those of previous PAGE studies on PpsR with the *puc* II sequence encompassing both binding motifs (17), but significantly lower than those determined by gel mobility shift assays for PpsR and a 262 bp *puc* promoter containing both binding sites (nM range, (17). That may be attributed to the ability of PpsR to interact with other components (e.g. AppA, heme). In order for these multiple interactions to take place, it may be essential that tight binding of any of these components is prohibited. Indeed, the dissociation constants for binding both AppA and heme are in the micromolar range: K_d of 1.3 μM for reduced AppA (17) and K_d of 2-4 μM for heme binding (Fig. S3D and (31)).

The affinity we observed for DNA1 (K_d =0.9 ±0.2 μM) is identical to that observed for full *puc* II by *Winkler et al*. (29) but higher than that of DNA2 (K_d = 5.3 ± 2.6 μM). Also, we did not observe evidence for mutual influence between DNA1 and DNA2 binding. Together, this suggests that the presence of the connecting sequence may be required to allow higher affinity DNA2 binding. Under our experimental conditions, we did not observe cooperativity effects in binding of PpsR to either DNA1 or DNA2. This is in contrast to the *puc* II experiments of *Winkler et al.* (29) and the *puc* experiments of *Masuda and Bauer* (17), suggesting that the separate motifs might not require octomerization of PpsR to bind. Altogether, given that DNA1 affinity is higher than DNA2 and similar to the full sequence affinity that requires an octamerization to bind, these results suggest that in the full *puc* II (or *puc*) sequence, oligomerization is initially triggered by binding of the DNA1 motif.

The effect of heme on DNA binding to PpsR

DNA binding is significantly affected by the presence of heme. As discussed above heme is able to form a complex with PpsR in the Fe(III) oxidation state, with His^{275} and Cys^{424} as the critical residues present in the PAS2 and HTH domains, respectively, that are able to bind to the heme iron. Gel mobility shift assays using the *puc* promoter that contains two PpsR binding sites located 8 bp apart, have shown that heme inhibits the ability of PpsR to form a higher-ordered PpsR-DNA complex. The same effect was also observed with different promoters, but the formation of the

PpsR-*puc* complex was more sensitive to disruption in the presence of heme (31). Footprint assays have confirmed the different conformations of the PpsR-*puc* complexes with and without bound heme (31). In line with these observations, our fluorescence studies have shown weaker binding of DNA both to PpsR and its truncated version, PAS2-HTH, in the presence of heme. In particular, we observed a ~10-fold increase in the dissociation constant K_d, for DNA1 binding in both heme-bound proteins. Heme is proposed to be accommodated in a cleft near Cys^{424} and a heme-induced conformational change in the protein may be responsible for this weaker DNA binding (28). One of the proposed mechanisms that control the strength of the DNA binding involves the oxidation-reduction of the disulphide bond between Cys^{424} in the HTH domain and Cys^{251} in the PAS1 domain of the protein. PpsR in the oxidized form (disulphide bridge present) has been shown to bind the *puc* DNA sequence approximately two times stronger *in vitro* compared to PpsR in the reduced form (free thiols) (17). Therefore, heme binding to Cys^{424} is expected to disrupt the disulphide bridge justifying the proposed conformational change and the decreased DNA affinity. Yet, the observed ~10-fold increase of the K_d of DNA binding in the presence of heme is significantly higher than the reported ~2-fold increase with reduced PpsR (and the lack of effect observed in our fluorescence anisotropy measurements with short DNA sequences, Fig. 6C and Fig. 6F) which suggests that other factors like occupation of the cleft where DNA binds nearby the heme may also be responsible. Whether the oxidation-reduction mechanism also has an effect on DNA binding *in vivo* remains to be investigated as *in vitro*, a trend of increasing DNA binding activity was observed by reduction of the disulphide bond (69). It should be noted that *in vivo* studies have shown that PpsR does not contain a disulphide bond either in aerobically or in anaerobically grown cells (69) at variance with an *in vitro* study that has shown that the disulphide bond of the oxidized PpsR can be formed in the presence of oxygen (10).

Disruption of the disulphide bridge upon heme binding to Cys^{424} could be considered analogous to the second mechanism reported to control the strength of DNA binding and that is the binding of AppA to PpsR. Reduced AppA has been shown to form a stable AppA-$PpsR_2$ complex (K_d of 1.3 μM) and to facilitate reduction of the disulphide bond in oxidized PpsR (17). In that complex, the apparent affinity of PpsR for *puc I* was slightly reduced with respect to that of PpsR in the absence of AppA (29). Our fluorescence anisotropy experiments on DNA binding to the AppA-PpsR complex are in general agreement with DNA binding data reported by Winkler et al. (29), only small effects on the presence of AppA were found on DNA binding (Fig. 6A and 6D).

Physiological implications and the role of heme in transcriptional regulation

PpsR, like a number of other transcriptional regulators, is a modular dimeric protein containing PAS domains and the effector domain HTH, which binds DNA. The heme molecule acts as the stimulus that binds to the PAS2 and HTH domains and induces conformational changes that are propagated via the amphipathic α-helical and coiled-coil linkers at the C termini of the core of PAS2 to the covalently attached DNA binding domain. We propose that at high oxygen levels heme iron in its ferric form coordinates weakly, partly via Cys^{424} (present in the HTH) and partly via His^{275} to PpsR, thus perturbing DNA binding, but without being able to dissociate DNA as indicated by our affinity measurements. As a result, the formation of the photosynthetic apparatus

is inhibited avoiding photooxidative stress (Fig. 7). However, we anticipate that at low oxygen levels, heme iron in its Fe(II) oxidation state displays a weak or no coordination with Cys^{424}, resulting in the formation of a five-coordinated species and a significant conformational change in the protein. That conformational change can affect the binding of DNA, which is able to dissociate and activate the expression of genes that encode components of the photosynthetic apparatus (Fig. 7). It should be noted that large conformational changes that take place upon DNA binding are a common characteristic of heme-binding gas-sensing transcriptional regulators like CooA (CO-sensing transcription activator from *Rhodospirillum rubrum*) (70) and DNR (dissimilative nitrate respiration regulator) (71). Ferrous heme binding to AppA may also induce conformational changes in the protein due to the weak binding to Cys^{231} affecting the interaction with PpsR. Future studies, under low oxygen levels in the presence of reducing agents able to reduce the heme iron are expected to shed more light in that direction.

It is quite surprising that heme is able to interact not only with PpsR, but also with AppA. This interaction is prone to provide another level of regulation for the formation of the photosynthetic apparatus. However, the role of heme in AppA remains controversial. Earlier studies have concluded that the AppA-PpsR regulatory system functions as an oxygen-dependent transcriptional rheostat. It was shown that oxygen can dissociate heme from AppA in a concentration-dependent manner (12). Subsequent studies favour a role of heme in controlling the amount of photosynthetic apparatus synthesized. It was shown that AppA can bind heme under both anaerobic and aerobic conditions. Based on the reduced length of the AppA photocycle upon heme binding, it was concluded that when heme was bound to the oxidized protein the population of AppA is higher in the dark state (21). Considering that only AppA in the dark state can bind to PpsR (21) -a finding that has been challenged (29)- heme binding favors the formation of the AppA-PpsR complex and hence promotes the biosynthesis of the photosynthetic apparatus. In this way it is ensured that there is a sufficient amount of heme available to handle the essential function of electron transfer (21). Based on these findings one could speculate that under blue light exposure and regardless of the oxygen levels, heme-bound AppA will favour the formation of the AppA-PpsR complex and hence the biosynthesis of the photosynthetic apparatus. By contrast, in the simultaneous presence of high oxygen levels and light, PpsR will remain bound to DNA and inhibit the formation of the photosynthetic apparatus and the associated photooxidative damage.

It should be noted that $AppA_{\Delta C}$ serves as a very good model for the full-length protein, but caution should be made in extrapolating results from $AppA_{\Delta C}$ to AppA. The Cys-rich domain although dispensable for oxygen sensing (12) has been reported to have a significant role in the interaction with PpsR. The not yet structurally solved redox-active cysteines in the Cys-rich domain of AppA are believed to reduce the redox active Cys in PpsR under anaerobic conditions and lower the DNA binding affinity of PpsR (17,72). The midpoint potential (E_m) of the redox active pair of cysteines in AppA is reported to be E_m= -325 mV (72) and to be very similar to the E_m=-320 mV potential of the disulphide pair in PpsR (17,72). The DNA binding affinity to PpsR seems to be affected slightly by the redox state of the two cysteines present in PAS1 and the not yet structurally solved HTH domain of PpsR (17). Similarly, the disulphide bridge (Cys^{399}-Cys^{406}, present in the Cys-rich

domain) in AppA has been reported to affect the heme binding properties of the SCHIC domain in the light-adapted state (21). In addition, in the presence of heme, the BLUF photocycle is significantly reduced in oxidized conditions and not affected in reduced conditions suggesting that the redox state of this disulphide bridge affects signal communication between the BLUF domain and the SCHIC domain (21).

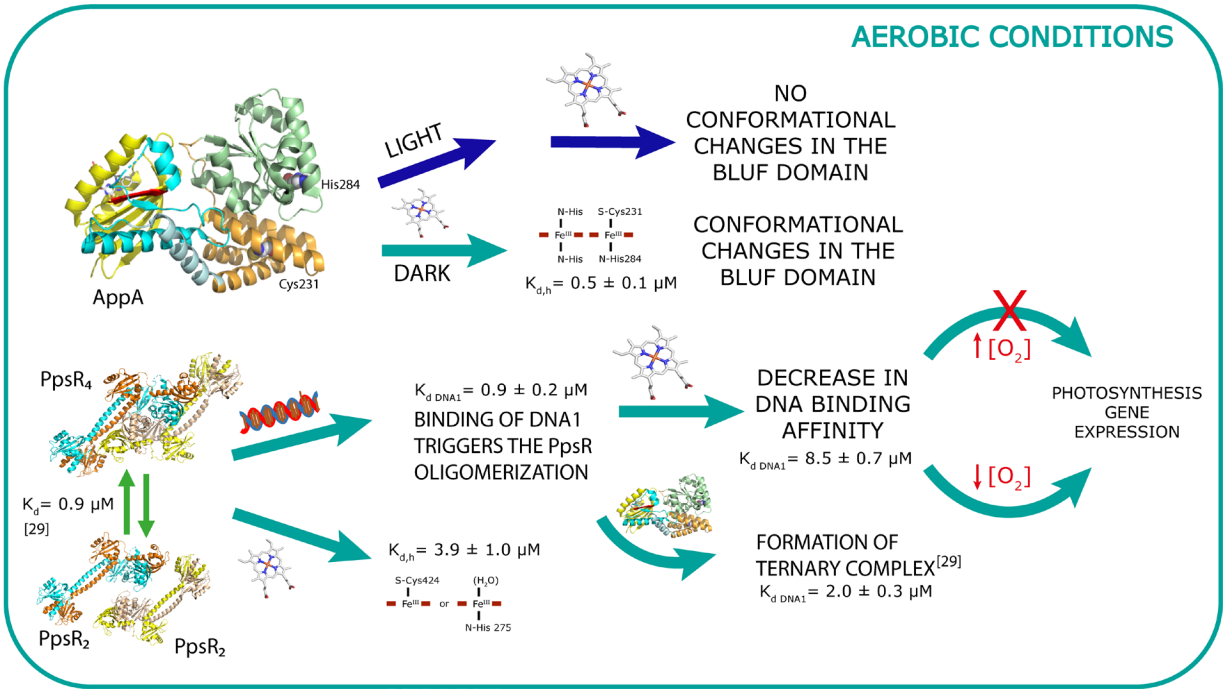

Fig. 7 Schematic diagram of the interaction of heme with AppA and PpsR in *Rhodobacter sphaeroides*. In the dark and under aerobic conditions heme interacts with AppA and induces conformational changes in the BLUF domain. On the contrary, under light conditions, changes in the SCHIC domain due to heme binding cannot be transmitted to the BLUF domain. Heme binding to PpsR decreases the DNA binding affinity to PpsR but at high oxygen concentration inhibits the gene expression of photosynthetic genes. At lower oxygen concentration, binding of ferrous heme is anticipated to result in conformational changes that release DNA and hence promotes the expression of photosynthetic genes.

Conclusion

Our study has provided further insight at the molecular level on the interaction of heme with the transcriptional regulatory system AppA/PpsR. It has revealed the involvement of cysteine residues in heme binding, a characteristic of heme regulated proteins using heme as a signalling molecule and conformational changes in the BLUF domain induced by heme binding to the 4HB-SCHIC domain of AppA. Besides this first level of signaling via its binding, heme can also provide a second level of signaling via the sensing of gases like oxygen. Study of the dynamics have revealed that allosteric interactions need to occur in both proteins in order for the light-signalling pathway to take place. Our study has also provided quantitative information on the individual DNA fragments of the *puc* promoter that bind to PpsR and has suggested that oligomerization of PpsR is initially triggered by binding of one of the two DNA fragments. Understanding the molecular

mechanism of the interaction of heme with PpsR and AppA will allow us to obtain a better understanding on an important component involved in the transcriptional regulation in *R. sphaeroides*. This knowledge may help us gain insight into this type of regulation in other biological systems with the ultimate goal to control gene expression which is a major challenge in the field of optogenetics.

Author Contributions

SMK, UL, MHV, AL; designed research, SMK, ZF, PD, MHV, AL; performed experiments, SMK, PD, MHV, AL; analysed data, PD, MHV, AL; obtained funding, SMK; wrote the manuscript with contributions from all authors; All authors read and approved the manuscript.

Sofia M. Kapetanaki https://orcid.org/0000-0003-1286-9929
Zsuzsanna Fekete https://orcid.org/0000-0002-4264-2365
Pierre Dorlet https://orcid.org/0000-0001-7394-3374
Marten H. Vos https://orcid.org/0000-0003-0493-4831
Ursula Liebl https://orcid.org/0000-0003-0869-4388
Andras Lukacs https://orcid.org/0000-0001-8841-9823

Acknowledgements

We thank Jinnette Tolentino Collado and Peter Tonge from Stony Brook University for the kind gift of the PpsR plasmid, Éva Hoffmanné Simon for excellent technical assistance and Jonatan Pasitka for helping with editing the figures. A.L. acknowledges funding from EFOP-3.6.2-16-2017-00005. A.L. and M.H.V. are grateful to the "Balaton" project (NKFIH 2017-2.2.5-TÉT-FR-2017-00005 and PHC Balaton 40173VE) for funding the travel exchanges. For EPR experiments, financial support from the IR INFRANALYTICS FR2054 for conducting the research is gratefully acknowledged.

Conflict of interest

The authors declare no conflict of interest

References

1. Shimizu T., A. Lengalova, V. Martinek, and M. Martinkova, 2019. Heme: emergent roles of heme in signal transduction, functional regulation and as catalytic centers. *Chem. Soc. Rev.* 48:5624-5657, doi:10.1039/C9CS00268E.
2. Gonzaga de França Lopes, L., F.S. Gouveia Júnior, A.K. Medeiros Holanda, I.M. Moreira de Carvalho, E. Longhinotti, T.F. Paulo, D.S. Abreu, P.V. Bernhardt, M-A. Gilles-Gonzalez, I.C. Nogueira Diógenes, and E.H. Silva Sousa, 2021. Bioinorganic systems

responsive to the diatomic gases O_2, NO, and CO: From biological sensors to therapy. *Coord. Chem. Rev*. 445:214096, doi:10.1016/j.ccr.2021.214096.

3. Gallio, A.E., S.S.-P. Fung, A. Cammack-Najera, A.J. Hudson, and E.L. Raven, 2021. Understanding the Logistics for the Distribution of Heme in Cells. *J. Am. Chem. Soc. Au* 1, 1541-1555, doi:10.1021/jacsau.1c00288.
4. White, C., X. Yuan, P.J. Schmidt, E. Bresciani, T.K. Samuel, D. Campagna, C. Hall, K. Bishop, M.L. Calicchio, A. Lapierre, D.M. Ward, P. Liu, M.D. Fleming, and I. Hamza, 2013. HRG1 is essential for heme transport from the phagolysosome of macrophages during erythrophagocytosis. *Cell Metab.* 17:261-270, doi:10.1016/j.cmet.2013.01.005.
5. Fleischhacker, A.S., and S.W. Ragsdale, 2018. An unlikely heme chaperone confirmed at last. *J. Biol. Chem.* 293:14569-14570, doi:10.1074/jbc.h118.005247.
6. Haskamp, V., S. Karrie, T. Mingers, S. Barthels, F. Alberge, A. Magalon, K. Müller, E. Bill, W. Lubitz, K. Kleeberg, P. Schweyen, M. Bröring, M. Jahn, and D. Jahn, 2018. The radical SAM protein HemW is a heme chaperone. *J. Biol. Chem*. 293:2558-2572, doi:10.1074/jbc.ra117.000229
7. Sweeny, E.A., A.B. Singh, R. Chakravarti, O. Martinez-Guzman, A. Saini, M.M. Haque, G. Garee, P.D. Dans, L. Hannibal, A.R. Reddi et al. 2018. Glyceraldehyde-3-phosphate dehydrogenase is a chaperone that allocates labile heme in cells. *J. Biol. Chem.* 293:14557-14568, doi:10.1074/jbc.ra118.004169.
8. Hanna, D.A., R.M. Harvey, O. Martinez-Guzman, X. Yuan, B. Chandrasekharan, G. Raju, F.W. Outten, I. Hamza, and A. Reddi, 2016. Heme dynamics and trafficking factors revealed by genetically encoded fluorescent heme sensors. *Proc. Natl. Acad. Sci. U. S. A.* 113:539-7544, doi:10.1073/pnas.1523802113.
9. Sassa, S., 2004. Why Heme Needs to Be Degraded to Iron, Biliverdin IXα, and Carbon Monoxide? *Antioxid. Redox Signal*, 6:819-824, doi:10.1089/ars.2004.6.819.
10. Zappa, S., K. Li, and C.E. Bauer, 2010. The tetrapyrrole biosynthetic pathway and its regulation in *Rhodobacter capsulatus*. *Adv. Exp. Med. Biol.* 675:229-250, doi:10.1007/978-1-4419-1528-3_13.
11. Chidgey, J.W., P.J. Jackson, M.J. Dickman, and C.N. Hunter, 2017. PufQ regulates porphyrin flux at the haem/bacteriochlorophyll branchpoint of tetrapyrrole biosynthesis via interactions with ferrochelatase. *Mol. Microbiol.* 106:961-975, doi:10.1111/mmi.13861.
12. Moskvin, O.V., S. Kaplan, M.A. Gilles-Gonzalez, and M. Gomelsky, 2007. Novel heme-based oxygen sensor with a revealing evolutionary history. *J. Biol. Chem.* 282:28740–28748, doi:10.1074/jbc.m703261200.
13. Gomelsky, M., and S. Kaplan, 1995. AppA, a novel gene encoding a trans-acting factor involved in the regulation of photosynthesis gene expression in *Rhodobacter sphaeroides*. *J. Bacteriol.* 177:4609-4618, doi:10.1128/jb.177.16.4609-4618.1995.
14. Gomelsky, M., and S. Kaplan, 1997. Molecular genetic analysis suggesting interactions between AppA and PpsR in regulation of photosynthesis gene expression in *Rhodobacter sphaeroides* 2.4.1. *J. Bacteriol*. 177:128-134, doi:10.1128/jb.179.1.128-134.1997.

15. Braatsch, S., and M. Gomelsky, 2004. Responses of the of the *Rhodobacter sphaeroides* transcriptome to blue light under semiaerobic conditions. *J. Bacteriol.* 186:7726–7735, doi:10.1128/jb.186.22.7726-7735.2004.
16. Shimada, H., K. Iba, and K. Takamiya, 1992. Blue-light irradiation reduces the expression of puf and puc operons of *Rhodobacter sphaeroides* under semi-aerobic conditions. *Plant Cell Physiol.* 33:471-475, doi:10.1093/oxfordjournals.pcp.a078276.
17. Masuda, S., and C.E. Bauer, 2002. AppA is a blue light photoreceptor that antirepresses photosynthesis gene expression in *Rhodobacter sphaeroides*. *Cell* 110:613–623, doi:10.1016/s0092-8674(02)00876-0.
18. Braatsch, S., M. Gomelsky, S. Kuphal, and G. Klug, 2002. A single flavoprotein, AppA, integrates both redox and light signals in *Rhodobacter sphaeroides*. *Mol. Microbiol.* 45:827–836, doi:10.1046/j.1365-2958.2002.03058.x.
19. Gomelsky, M., and G. Klug, 2002. BLUF: A novel FAD-binding domain involved in sensory transduction in microorganisms. *Trends Biochem. Sci.* 27:497–500, doi:10.1016/s0968-0004(02)02181-3.
20. Han, Y., M.H.F. Meyer, M. Keusgen, and G. Klug, 2007. A haem cofactor is required for redox and light signalling by the AppA protein of *Rhodobacter sphaeroides*. *Mol. Microbiol.* 64:1090-1104, doi:10.1111/j.1365-2958.2007.05724.x.
21. Yin, L., V. Dragnea, G. Feldman, L.A. Hammad, J.A. Karty, C.E. Dann III, and C.E. Bauer, 2013. Redox and light control the heme-sensing activity of AppA. *MBio* 4:1–9, doi.org/10.1128/mbio.00563-13.
22. Karadi, K., S.M. Kapetanaki, K. Raics, I. Pecsi, R. Kapronczai, Z. Fekete, J.N. Iuliano, J. Tolentino Collado, A. Gil, J. Orban et al., 2020. Functional dynamics of a single tryptophan residue in a BLUF protein revealed by fluorescence spectroscopy. *Sci. Rep.* 10:2061, doi.org/10.1038/s41598-020-59073-5.
23. Gomelsky, M., and S. Kaplan, 1995. Genetic evidence that PpsR from *Rhodobacter Sphaeroides* 2.4.1 functions as a repressor of *puc* and *bchf* expression. *J. Bacteriol.* 177: 1634-1637, doi:10.1128/jb.177.6.1634-1637.1995.
24. Lee, J.K., P.J. Kiley, and S. Kaplan, 1989. Posttranscriptional control of puc operon expression of B800-850 light-harvesting complex formation in *Rhodobacter sphaeroides J. Bacteriol.* 171:3391-3405, doi:10.1128/jb.171.6.3391-3405.1989.
25. Elsen, S., M. Jaubert, D. Pignol, E. Giraud, 2005. PpsR: A multifaceted regulator of photosynthesis gene expression in purple bacteria. *Mol Microbiol* 57:17–26, doi:10.1111/j.1365-2958.2005.04655.x.
26. Yamazaki, Y., H. Fukusumi, H. Kamikubo, M. Kataoka, 2008. Role of the N-terminal region in the function of the photosynthetic bacterium transcription regulator PpsR. *Photochem. Photobiol*. 84:839–844, doi:10.1111/j.1751-1097.2008.00306.x.
27. Moskvin, O.V., L. Gomelsky, and M. Gomelsky, 2005. Transcriptome analysis of the *Rhodobacter sphaeroides* PpsR regulon: PpsR as a master regulator of photosystem development. *J. Bacteriol.* 187:2148–2156, doi:10.1128/jb.187.6.2148-2156.2005.

28. Gomelsky, M., I.M. Horne, H-J. Lee, J.M. Pemberton, A.G. McEwan, and S. Kaplan, 2000. Domain structure, oligomeric state, and mutational analysis of PpsR, the *Rhodobacter sphaeroides* repressor of photosystem gene expression. *J. Bacteriol.* 182:2253-2261, doi:10.1128/jb.182.8.2253-2261.2000.
29. Winkler, A., U. Heintz, R. Lindner, J. Reinstein, R.L. Shoeman, and I. Schlichting, 2013. A ternary AppA-PpsR-DNA complex mediates light regulation of photosynthesis-related gene expression. *Nat. Struct. Mol. Biol.* 20:859–867, doi:10.1038/nsmb.2597.
30. Cournac, A., and J. Plumbridge, 2013. DNA Looping in Prokaryotes: Experimental and Theoretical Approaches. *J. Bacteriol.* 195:1109-1119, doi:10.1128/jb.02038-12.
31. Yin, L., V. Dragnea, and C.E. Bauer, 2012. PpsR, a regulator of heme and bacteriochlorophyll biosynthesis, is a heme-sensing protein. *J. Biol. Chem.* 287:13850–13858, doi:10.1074/jbc.m112.346494.
32. Dawson RMC, Elliot DC, Elliot WH, Jones KM (1975) Data for Biochemical Research. pp 230-231. Oxford: Oxford University Press
33. Morrison, J.F., 1969. Kinetics of the reversible inhibition of enzyme-catalysed reactions by tight-binding inhibitors. *Biochim. Biophys. Acta* 18:269-286. doi:10.1016/0005-2744(69)90420-3.
34. Jäger, A., S. Braatsch, K. Haberzettl, S. Metz, L. Osterloh, Y. Han, G. Klug, 2007. The AppA and PpsR Proteins from *Rhodobacter sphaeroides* Can Establish a Redox-Dependent Signal Chain but Fail to Transmit Blue-Light Signals in Other Bacteria. *J. Bacteriol.* 189:2274–2282. doi:10.1128/jb.01699-06.
35. Lakowicz. J. R. Principles of Fluorescence Spectroscopy (2006) Springer
36. Valeur, B (2001) Molecular Fluorescence: Principles and applications (Wiley-VCH Verlag GmbH)
37. Olson, J.S., E.W. Foley, D.H. Maillett, and E.V. Paster, 2003. Measurement of rate constants for reactions of O_2, CO, and NO with hemoglobin. *Methods Mol. Med.* 82:65-91, doi:10.1385/1-59259-373-9:065.
38. Nag, L., A. Lukacs, and M.H. Vos, 2019. Short-Lived Radical Intermediates in the Photochemistry of Glucose oxidase. *ChemPhysChem* 20:1793-1798, doi:10.1002/cphc.201900329.
39. Snellenburg, J.J., S.P. Laptenok, R. Seger, K.M. Mullen, and I.H.M. van Stokkum, 2012. Glotaran: A Java-Based Graphical User Interface for the R Package TIMP. *J. Stat. Softw.* 49:1–22, doi:10.18637/jss.v049.i03.
40. Blumberg, W.E. and J. Peisach, 1971. Low-Spin Compounds of Heme Proteins In Bioinorganic Chemistry, American Chemical Society: Vol. 100, pp 271-291, doi:10.1021/ba-1971-0100.ch013.
41. Smith, A.T., S. Pazicni, K. Marvin, D.J. Stevens, K. Paulsen, and J.N. Burstyn, 2015. Functional divergence of heme-thiolate proteins: A classification based on spectroscopic attributes *Chem. Rev*. 115:2532-2558, doi:10.1021/cr500056m.
42. Vos, M.H., 2008. Ultrafast dynamics of ligands within heme proteins. *BBA Bioenergetics*

1777:15–31, doi:10.1016/j.bbabio.2007.10.004.
43. Petrich, J.W., C. Poyart, J.L. Martin, 1988. Photophysics and reactivity of heme proteins: a femtosecond absorption study of hemoglobin, myoglobin, and protoheme. *Biochemistry* 27, 4049-4060, doi:10.1021/bi00411a022.
44. Salman, M., C. Villamil Franco, R. Ramodiharilafy, U. Liebl, and M.H. Vos, 2019. Interaction of the full-length heme-based CO sensor protein RcoM-2 with ligands. *Biochemistry* 58:4028–4034, doi:10.1021/acs.biochem.9b00623.
45. Benabbas, A., V. Karunakaran, H. Youn, T.L. Poulos, and P.M. Champion, 2012. Effect of DNA binding on geminate CO recombination kinetics in CO-sensing transcription factor CooA. *J. Biol. Chem.* 287:21729–21740, doi:10.1074/jbc.m112.345090.
46. Kumazaki, S., H. Nakajima, T. Sakaguchi, E. Nakagawa, H. Shinohara, K. Yoshihara, and S. Aono, 2000. Dissociation and recombination between ligands and heme in a CO-sensing transcriptional activator CooA: A flash photolysis study. *J. Biol. Chem.* 275:38378–38383, doi:10.1074/jbc.m005533200.
47. Lobato, L., L. Bouzhir-Sima, T. Yamashita, M.T. Wilson, M.H. Vos, and U. Liebl, 2014. Dynamics of the heme-binding bacterial gas-sensing Dissimilative Nitrate Respiration Regulator (DNR) and activation barriers for ligand binding and escape. *J. Biol. Chem.* 289: 26514–26524, doi:10.1074/jbc.m114.571398.
48. Liebl, U., L. Bouzhir-Sima, L. Kiger, M.C. Marden, J.C. Lambry, M. Negrerie, and M.H. Vos, 2003. Ligand binding dynamics to the heme domain of the oxygen sensor Dos from *Escherichia coli*. *Biochemistry* 42:6527–6535, doi:10.1021/bi027359f.
49. Lechauve, C., L. Bouzhir-Sima, T. Yamashita, M.C. Marden, M.H. Vos, U. Liebl, and L. Kiger, 2009. Heme Ligand Binding Properties and Intradimer Interactions in the Full-length Sensor Protein Dos from *Escherichia coli* and Its Isolated Heme Domain *J. Biol. Chem.* 284:36146-36159, doi:10.1074/jbc.m109.066811.
50. Liebl, U., L. Bouzhir-Sima, M. Negrerie, J-L. Martin, and M.H. Vos, 2002. Ultrafast ligand rebinding in the heme domain of the oxygen sensors FixL and Dos: general regulatory implications for heme-based sensors *Proc. Natl. Acad. Sci. U.S.A.* 99:12771, doi:10.1073/pnas.192311699.
51. Jasaitis, A., K. Hola, L. Bouzhir-Sima, J-C. Lambry, V. Balland, M.H. Vos, and U. Liebl, 2006. Role of distal arginine in early sensing intermediates in the heme domain of the oxygen sensor FixL. *Biochemistry* 45:6018–6026, doi:10.1021/bi060012i.
52. Bouzhir-Sima, L., R. Motterlini, J. Gross, M.H. Vos, and U. Liebl, 2016. Unusual Dynamics of Ligand Binding to the Heme Domain of the Bacterial CO Sensor Protein RcoM-2. *J Phys Chem B* 120:10686–10694, doi:10.1021/acs.jpcb.6b08160.
53. Kapetanaki, S.M., M.J. Burton, J. Basran, C. Uragami, P.C.E. Moody, J.S. Mitcheson, R. Schmid, N.W. Davies, P. Dorlet, M.H. Vos et al., 2018. A mechanism for CO regulation of ion channels. *Nat. Commun.* 9:907, doi:10.1038/s41467-018-03291-z.

54. Yoshimura, T., S. Suzuki, A. Nakahara, H. Iwasaki, M. Masuko, and T. Matsubara, 1986. Spectral properties of nitric oxide complexes of cytochrome c' from Alcaligenes sp. NCIB 11015. *Biochemistry* 25:2436-2442, doi:10.1021/bi00357a021.
55. Stone, J.R., M.A. Marletta, 1994. Soluble guanylate cyclase from bovine lung: activation with nitric oxide and carbon monoxide and spectral characterization of the ferrous and ferric states. *Biochemistry* 33:5636-5640, doi:10.1021/bi00184a036.
56. Reynolds, M.F., R.B. Parks, J.N. Burstyn, D. Shelver, M.V. Thorsteinsson, R.L. Kerby, G.P. Roberts, K.M. Vogel, and T.G. Spiro, 2000. Electronic Absorption, EPR, and Resonance Raman Spectroscopy of CooA, a CO-Sensing Transcription Activator from *R. rubrum*, Reveals a Five -Coordinate NO- Heme. *Biochemistry* 39: 388-396, doi:10.1021/bi991378g.
57. Taoka ,S., and R. Banerjee, 2001. Characterization of NO binding to human cystathione beta-synthase: possible implications of the effects of CO and NO binding to the human enzyme. *J. Inorg. Biochem.* 87:245-251, doi:10.1016/s0162-0134(01)00335-x.
58. Silkstone, G., S.M. Kapetanaki, I. Husu, M.H. Vos, and M.T. Wilson, 2010. Nitric oxide binds to the proximal heme coordination site of the ferrocytochrome c/cardiolipin complex: formation mechanism and dynamics. *J. Biol. Chem.* 285:19785-19792, doi:10.1074/jbc.m109.067736.
59. Igarashi, J., A. Sato, T. Kitagawa, T. Yoshimura, S. Yamauchi, I. Sagami, T. Shimizu, 2004. Activation of heme-regulated eukaryotic initiation factor 2alpha kinase by nitric oxide is induced by the formation of a five -coordinate NO-heme complex: optical absorption, electron spin resonance, and resonance raman spectral studies. *J. Biol. Chem.* 279:15752-15762, doi:10.1074/jbc.m310273200.
60. Brazard, J., A. Usman, F. Lacombat, C. Ley, M.M. Martin, and P. Plaza, 2011. New insights into the ultrafast photophysics of oxidized and reduced FAD in solution. *J. Phys. Chem. A* 115:3251–3262, doi:10.1021/jp110741y.
61. Leenders,H.R., J. Vervoort, A. van Hoek, and A.J. Visser, 1990. Time-resolved fluorescence studies of flavodoxin. Fluorescence decay and fluorescence anisotropy decay of tryptophan in Desulfovibrio flavodoxins. *Eur. Biophys. J.* 18:43–55, doi:10.1007/bf00185419.
62. Leenders, R., A. Van Hoek, M. Van Iersel, C. Veeger, and A.J. Visser, 1993. Flavin dynamics in oxidized Clostridium beijerinckii flavodoxin as assessed by time-resolved polarized fluorescence. *Eur. J. Biochem.* 218:977–984, doi:10.1111/j.1432-1033.1993.tb18456.x.
63. Krasnopevtseva, M.K., V.P. Belik, I.V. Semenova, A.G. Smolin, A.A. Bogdanov, and O.S. Vasyutinskii, 2020. Decay Times and Anisotropy in Polarized Fluorescence of Flavin Adenine Dinucleotide Determined with Subnanosecond Resolution. *Tech. Phys. Lett.* 46, 614–616, doi:10.1134/S1063785020060218.
64. Jäger, A., S. Braatsch, K. Haberzettl, S. Metz, L. Osterloh, Y. Han, and G. Klug, 2007. The AppA and PpsR Proteins from *Rhodobacter sphaeroides* Can Establish a Redox-

Dependent Signal Chain but Fail to Transmit Blue-Light Signals in Other Bacteria. *J. Bacteriol*. 189:2274–2282, doi:10.1128/jb.01699-06.

65. Miksanova, M., J. Igarashi, M. Minami, I. Sagami, S. Yamauchi, H. Kurokawa, and T. Shimizu, 2006. Characterization of Heme-Regulated eIF2R Kinase: Roles of the N-Terminal Domain in the Oligomeric State, Heme Binding, Catalysis, and Inhibition *Biochemistry* 45:9894-9905, doi:10.1021/bi060556k.
66. Shimizu, T., 2012. Binding of cysteine thiolate to the Fe(III) heme complex is critical for the function of heme sensor proteins. *J. Inorg. Biochem.* 108:171-177, doi:10.1016/j.jinorgbio.2011.08.018.
67. Liebl, U., J.C. Lambry, and M.H. Vos, 2013. Primary processes in heme-based sensor proteins. *Biochimica et Biophysica Acta - Proteins Proteomics* 1834:1684–1692, doi:10.1016/j.bbapap.2013.02.025.
68. Youn, H., M.V. Thorsteinsson, M. Conrad, R.L. Kerby, and G.P. Roberts, 2005. Dual roles of an E-Helix, Glu167, in the Transcriptional Activator Function of CooA. *J. Bacteriol.* 187: 2573-2581, doi:10.1128/jb.187.8.2573-2581.2005.
69. Cho, S.-H., S.-H. Youn, S.-R. Lee, H.-S. Yim, and S.-O. Kang, 2004. Redox property and regulation of PpsR, a transcriptional repressor of photosystem gene expression in *Rhodobacter sphaeroides. Microbiology* 150:697-705, doi:10.1099/mic.0.26777-0.
70. Roberts, G.P., R.L. Kerby, H. Youn, M. Conrad, 2005. CooA, a paradigm for gas sensing regulatory proteins. *J. Inorg. Biochem.* 99:280-292, doi:10.1016/j.jinorgbio.2004.10.032.
71. Giardina, G., S. Rinaldo, N. Castiglione, M. Caruso, and F. Curtuzzola, 2009. A dramatic conformational rearrangement is necessary for the activation of DNR from *Pseudomonas aeruginosa*. Crystal structure of wild-type DNR. *Proteins* 77:174-180, doi:10.1002/prot.22428.
72. Kim, S.K., J.T. Mason, D.B. Knaff, C.E. Bauer, and A.T. Setterdahl, 2006. Redox properties of the *Rhodobacter sphaeroides* transcriptional regulatory proteins PpsR and AppA. *Photosynth. Res.* 89:89-98, doi:10.1007/s11120-006-9086-4.